ANALYTIC
1 of 1
61 P.

IN - 18339

MMIC DEVICES FOR ACTIVE PHASED ARRAY ANTENNAS

FINAL REPORT

Supported by

Contract No. NASA NCC3-8
National Aeronautics and Space Administration
Lewis Research Center
Cleveland, Ohio 44135

July 31, 1986

(NASA-CR-176990) MMIC DEVICES FOR ACTIVE PHASED ARRAY ANTENNAS Final Report (Illinois Univ.) 61 p CSCL 20N
N86-30037 THRU N86-30038
Unclas
G3/32 43498

by

R. Mittra
Electromagnetic Communication Laboratory
Department of Electrical and Computer Engineering
University of Illinois
Urbana, Illinois 61801

ABSTRACT

In this report we investigated the use of finlines for microwave monolithic integrated circuit application in 20-30 GHz frequency range. Other wave guiding structures, e.g., microstrip lines are also examined from a comparative point of view and some conclusions are drawn on the basis of the results of the study.

I. INTRODUCTION

Current microwave technology allows the fabrication of many active devices operating [1] in the 20-30 GHz frequency range, and continuous improvement in the performance of these devices is predicted in the future. The integration of these devices into a monolithic configuration is a challenging problem and will require the development of new techniques for analyzing the MMIC circuits. In this study we evaluate a number of waveguide media including the finline which appears to hold good promise for integration of the active devices. The substrate dielectric considered is GaAs since it gives good performance at these frequencies, and technique for fabricating GaAs are widely available.

Several integrated waveguides have been considered in the literature for MMIC application. These include microstrip, finline, coplanar waveguide, suspended microstrip and hybrid combinations of these. Some of the guiding structures mentioned above are not very compatible with three terminal devices ices and hence are not considered as prime candidates.

Microstrip has been the favorite at lower microwave frequencies and has, in fact, found some applications up to the 100 GHz range. At higher frequencies the losses in microstrip lines become significant and, in the case of unshielded microstrip, the continuous spectrum of modes causes radiation problems at discontinuities, etc. Shielded microstrip avoids some of these difficulties, but the shield may not be amenable to integration. Suspended microstrip has lower loss than regular microstrip and is shown in Fig. 1.

The unilateral finline configuration is shown in Fig. 2. Here the slot acts as the guiding structure. Finline has potentially lower loss and better modal characteristics than microstrip. The dominant finline mode has a low frequency cut-off (unlike microstrip), and over the frequency range of operation the shield dimensions are usually such that only the dominant mode propagates. Bilateral finline has identical metalization on both sides of the dielectric. Antipodal finline is shown in Fig. 3 and will be discussed in relation to the amplifier.

Coplanar waveguide, which is shown in Fig. 4, has potential for millimeter-wave integrated circuits. Appendix A-C include some papers dealing with coplanar.

Theoretical data for finline, which is considered to be a prime candidate for integration with a GaAs substrate, is presented in Section 2.1. A brief discussion of the problem formulation and numerical solution are given. Section 2.2 indicates some methods for solving various discontinuity problems which occur in the amplifier (i.e., solution of the three-dimensional problem). Section 3 provides a relative assessment of the finline technology, along with recommendations.

2. FINLINE ANALYSIS

2.1. Uniform Finline

The uniform fin-line structure may be analyzed by using a spectral domain formulation with a moment method solution. Phase constant, mode function and characteristic impedance data may thus be obtained. Waveguides of this form are most simply formulated in the spectral domain, which involves using a Fourier series representation of all field quantities in the transverse direction, parallel to the metallization (i.e., the x-direction) [2]-[12]. Consider a spectral variable k_x, which has discrete values given by $k_x = 2n\ \pi/2b$. The fin-line modes are superpositions of TE - to - y and TM - to - y modes. Decoupled transverse resonance equations may be obtained by using a coordinate transformation in the (x,z) plane [6]. This allows use of transmission line equivalent circuits, which require only minor alterations to be applicable to other, perhaps more complex, geometries. This analysis results in a type of dyadic Green's function relationship in the spectral domain, relating slot fields to fin currents in the plane of the metallization. This relationship may be written in the form

$$\begin{bmatrix} Y_{xx} & Y_{xz} \\ Y_{zx} & Y_{zz} \end{bmatrix} \begin{bmatrix} \tilde{E}_x \\ \tilde{E}_z \end{bmatrix} = \begin{bmatrix} \tilde{J}_z \\ \tilde{J}_z \end{bmatrix} \tag{1}$$

A moment method, namely Galerkin's method, where the testing and basis functions are the same, may be used to obtain a satisfactory numerical solution to Eq. 1. The fields are expressed as

$$E_x(x) = \sum_{p=1}^{P} a_p \, \zeta_p(x) \tag{2a}$$

$$E_z(x) = \sum_{q=1}^{Q} b_q \, \eta_q(x). \tag{2b}$$

A suitable set of basis functions is an orthogonal set of functions, e.g., trigonometric functions or Chebyshev polynomials, modified b y an edge condition. With the orthogonality of $\zeta_p(x)$ and $\eta_q(x)$ with $\tilde{J}(x)$, a homogeneous equation of the form Lf = 0 results, where f is the unknown containing the coefficients of the basis functions. The numerical solution of the determinantal equation yields the eigenvalue solutions, or phase constants, for both propagating and evanescent modes. The solution for the slot fields can then be obtained by solving the matrix equation for the relative coefficients of the basis functions. The mode functions can be determined by returning to the transverse resonance analysis. The characteristic impedance may be defined by

$$Z_o = \frac{|V_x|^2}{2P} \tag{3}$$

where V_x is the slot voltage and P the mode power. The mode power is determined from the transverse resonance analysis. Theoretical results for the phase constants and characteristic impedances are given in [6]-[12] and mode functions in [8]. It should be noted that this definition for the characteristic impedance is considered a reasonable representation of the physical quantity. However, the measured characteristic impedance could differ and this aspect needs to be investigated experimentally.

The fields for the *nth* mode may be expressed as

$$\bar{E}(x,y,z) = \bar{e}_n(x,y)e^{-jk_{zn}z} + \bar{e}_{zn}(x,y)e^{-jk_{zn}z} \tag{4a}$$

$$\bar{H}(x,y,z) = \bar{h}_n(x,y)e^{-jk_{nz}z} + \bar{h}_{zn}(x,y)e^{-jk_{zn}z} \tag{4b}$$

where $\bar{e}_n$ and $\bar{h}_n$ are transverse vector mode functions, and $\bar{e}_{zn}$ and $\bar{h}_{zn}$ are the longitudinal vector mode functions. These mode functions, when normalized, satisfy the following orthogonality relationship

$$\int_{\infty}\int \bar{e}_n \times \bar{h}_m \cdot \hat{z}\, ds = \delta_{nm} \tag{5}$$

where δ_{nm} is the Kronecker delta.

Two well chosen basis functions, with greater than 16 b/w spectral terms in the inner product operation used to obtain the matrix equation, provide reasonable accuracy in the phase constants. However, a larger number of spectral terms and/or basis functions are required to obtain satisfactory approximations for the fields or mode functions. It is quite difficult to obtain a satisfactory representation for the propagating and evanescent mode functions. In fact, the orthogonality relationship of Eq. (5) is satisfied only approximately by one propagating and about two evanescent modes, when using two and four basis functions and a sufficient number of spectral terms to obtain convergence. Therefore, although an infinite number of approximate solutions can be obtained, only the first few such solutions are likely to be useful.

The computed finline data for normalized wavelength is shown in Figs. 5-9 and the characteristic impedance is given in Fig. 10. Figure 5 gives the wavelength for the propagating modes as a function of frequency and slot width. Figures 5-9 give the propagating and first evanescent mode. Two basis functions for E_x and E_z were used. These functions are

$$\zeta_p(x) = \frac{\cos\left[\frac{(p-1)\pi}{w}\left(x - s - \frac{w}{2}\right)\right]}{1 - \left[\frac{2(x-s)}{w}\right]^2}, \quad p = 1,2,3,\ldots$$

$$s - \frac{w}{2} < x < s + \frac{w}{2} \tag{6}$$

$$\eta_q(x) = \frac{\sin\left[\frac{q\pi}{w}\left(x - s - \frac{w}{2}\right)\right]}{1 - \left[\frac{2(x-s)}{w}\right]^2}, \quad q = 1,2,3,\ldots$$

$$\left.\begin{aligned}\zeta_p(x) &= 0\\ \eta_z(x) &= 0\end{aligned}\right\} \textit{otherwise}$$

and $\zeta_0(x) = P_x(s,w)$, where $P_x(s,w)$ is a pulse function of width w centered at $x = s$. One

hundred spectral terms were used in the evaluation of the matrix for the eigenvalue problem. Two hundred spectral terms were used to calculate the basis function coefficients and the characteristic impedances. It should be noted that more spectral terms are required for convergence of the fields than are required for convergence in the phase constants.

2.2. Discontinuity Analysis

The monolithic integrated waveguide structure, whether it be finline, microstrip or some other planar geometry, has a number of discontinuities which need to be characterized. Several suggested configurations are proposed in Section 3. All involve some type of low-reflection transition from rectangular waveguide to the uniform integrated line, and typically some form of matching to the FET. The matching could take on a variety of forms, all of which involve a series of discontinuities. It is thus evident that the analysis of several classes of discontinuities is crucial in the design and evaluation of the amplifier.

We have been studying such a class of problems for a number of years. The basic problem and numerical solution is essentially independent of the particular waveguide under consideration. Hence, generally a solution for one type of waveguide (for example microstrip) could equally well be applied to another in the same family (for example finline).

A common discontinuity in microstrip is a perturbation in the strip width, for example a step change. A number of such discontinuities occur in high-speed digital, microwave and millimeter-wave circuits. Discontinuities form the basis of filter and matching structures. The accurate solution of this class of problems is essential for the analysis and design of many components.

Formulations for the discontinuity problem may be classified into two categories:

(a) those that employ a representation for the unknown over the transverse junction plane, and

(b) those that utilize unknowns in the plane of the metallization.

These approaches will now be outlined.

Approach (a) relies on the construction of the Green's function using modal solutions. Included in this category are the mode matching solutions [10], [13]-[16]. The unknown quantities may be represented by a magnetic current ($\overline{K}$) in the transverse junction plane, leading to an integral equation formulation. A solution of this integral equation can then be obtained by an appropriate numerical method. Iterative and variational techniques for the solution of $\overline{K}$ have been investigated by this researcher [17]-[19]. Some success has been achieved with these approaches. However, the inherent limitation is the difficulty of obtaining accurate numerical solutions for the higher order modes [11]. More satisfactory approaches are currently under consideration.

The advantage of approach (b) is that it uses a spectral Green's function which is exact. This approach is basically an extension of the two-dimensional analysis (one-dimensional spectral relationship) of Section 2.1. The three-dimensional scattering problem is thus reduced to a two-dimensional spectral relationship in the plane of the strip [9]. The spectral variable k_x takes on the same values as in the uniform case, and k_z is continuous in general. For an infinite periodic structure, k_z is discrete. We are continuing to study [20] several formulations and numerical methods suitable for this approach. The major difficulties are associated with the problem containment to a finite z-support, the evaluation of the two-dimensional inner products, and the number of functions required to adequately represent the unknown.

3. COMPARATIVE ASSESSMENT OF TECHNOLOGIES FOR AMPLIFIER REALIZATION

For the purposes of further research it is important to assess the relative merits of a finline for use in the 20-30 GHz. The finline configuration is therefore compared with microstrip and other possible candidates so as to give some insight into the selection.

Finline has definite advantages over microstrip in that it has a lower loss and does not suffer from radiation problems. The finline structure is generally operated in the single mode region, which means that coupling to other propagating/leaky modes will not occur at discontinuities.

Unfortunately, it is difficult to incorporate a three-terminal device into finline. Several possible configurations are shown in Fig. 11. The geometry of Fig. 11(a) consists of a combination of unilateral and antipodal finline. Figure 11(b) shows an alternative which is a combination of unilateral finline and microstrip. The production of a suitable transition from rectangular waveguide to finline and the discontinuity, such as an exponential taper [21] is important. The abrupt step in the fin metallization at the FET in the configuration of Fig. 11(a) is of concern. It may be possible to compensate via appropriate matching, which should be verified experimentally. This matching may not be able to compensate for the finline discontinuity susceptance at the device, which is a higher order evanescent mode phenomena. Test structures for evaluation purposes could easily be fabricated on alumina substrates (alumina has a dielectric constant of approx. 9.6, which will give insight to the GaAs performance). The structure in Fig. 11(a) comprises unilateral and antipodal finline. One can reasonably draw conclusions regarding the antipodal structure, without having pursued the computation, by noting that the fin current distribution is similar to the unilateral case. It can be expected that the phase constants and characteristic impedance of the antipodal form would not differ greatly from the unilateral case.

The microstrip geometry is more compatible with three terminal devices. For a WR-28 test arrangement, a satisfactory transition to microstrip is required. Possible rectangular waveguide to microstrip transitions are shown in Fig. 12. The ridged waveguide transition is illustrated in Figs. 13-15. The van Heuven transition [22], [23] is shown conceptually in Figs. 16 and 17. The van Heuven transition appears to work quite well and can be easily fabricated.

The use of coplanar waveguide structure, which is shown in Fig. 4, may provide a viable low-loss alternative to finline. Coplanar waveguide provides three signal conductor planes and therefore would be compatible with three terminal components. The modal character in the unshielded guide may be troublesome, as in the unshielded microstrip case. An alternative which avoids this problem is shielded coplanar waveguide. Coplanar to microstrip transitions have been produced [24], [25]. Such transitions to microstrip may be useful in the vicinity of the device.

The rectangular waveguide to finline transition often consists of a non-linear taper of the metallization and then a tapering of the dielectric (the latter would not be the case with a GaAs substrate due to fabrication difficulties). Such a continuous transition can be modeled by a series of steps in the slot width. Step changes in the slot width also appear in matching and filter structures. Solutions to these problems could be obtained by one of several methods as described in categories (a) and (b):

- mode matching with discrete steps in the slot width
- "quasi" mode matching using approximate model solutions as basis functions (modal orthogonality is not used here)
- formulation with unknowns in the metalized planes

The continuous transition could be modeled by using the concept of a slowly varying parameter, namely the slot width. The application of these approaches would be valuable longer-term research activities. There are a number of important problems in the monolithic amplifier geometries, the solutions of which will require innovative formulations and numerical solutions.

It is suggested that further investigation of both a microstrip and a finline amplifier be carried out. The microstrip amplifier could easily be realized with a van Heuven transition, and in the vicinity of the FET the geometry is well known. In the finline case, the tapered rectangular waveguide to finline transition performs satisfactorily. The basic geometry for the finline amplifier could be the unilateral/antipodal geometry or the microstrip finline configuration. The possibility of incorporating coplanar waveguide as an alternative to finline should be investigated further. The experimental investigation of both the passive and active circuits will yield results to compliment this study and to permit the most satisfactory technology to be selected.

REFERENCES

[1] Y. H. Yun et. al., "Ka-band GaAs power FET's," 1983 IEEE MTT-S *International Microwave Symposium Digest*, pp. 136-138.

[2] T. Itoh and R. Mittra, "A technique for computing dispersion characteristics of shielded microstrip lines," *IEEE Trans. Microwave Theory Tech.*, vol. MTT-22, pp. 896-898, October 1974.

[3] D. Mirshekar-Syahkal, "An accurate determination of dielectric loss effects in monolithic microwave integrated circuits including microstrip and coupled microstrip," *IEEE Trans. Microwave Theory Tech.*, vol. MTT-31, pp. 950-954, November 1983.

[4] T. Itoh, "Spectral domain immittance approach for dispersion characteristics of generalized printed transmission lines," *IEEE Trans. Microwave Theory Tech.*, vol. MTT-28, pp. 733-736, July 1980.

[5] R. Jansen, "Unified user-oriented computation of shielded, covered and open planar microwave and millimeter-wave transmission characteristics," *IEE Proc. Pt. H, Microwaves Opt. Acoust.*, vol. MOA 1, pp. 14-22, 1979.

[6] L. Schmidt and T. Itoh, "Spectral domain analysis of dominant and higher order modes in fin lines," *IEEE Trans. Microwave Theory Tech.*, vol. MTT-38, pp. 981-985, September 1980.

[7] L. Schmidt, T. Itoh, and H. Hofmann, "Characteristics of unilateral fin-line structures with arbitrarily located slots," *IEEE Trans. Microwave Theory Tech.*, vol. MTT-29, pp. 352-355, April 1981.

[8] K. J. Webb and R. Mittra, "An overview of the spectral domain analysis of fin-line discontinuities using the method of moments," *Proc. IEEE AP/MTT-S 5th Annual Benjamin Franklin Symposium on Advances in* Antenna and Microwave Technology, Philadelphia, PA, pp. 64-66, May 8, 1985.

[9] K. Webb, "Investigation of planar waveguides and components for millimeter-wave integrated circuits," Ph.D. thesis, University of Illinois, Urbana, 1984.

[10] E. G. Farr, "An investigation of modal characteristics and discontinuities in printed circuit transmission lines," Ph.D. thesis, University of Illinois, Urbana, 1985.

[11] K. J. Webb, E. G. Farr and R. Mittra, "A note on the numerical solution for fin-line and microstrip modes," to appear in the *IEEE Trans. Microwave Theory Tech.*

[12] T. Itoh, "Generalized spectral domain method for multiconductor printed lines and its application to tunable suspended microstrips," *IEEE Trans. Microwave Theory Tech.*, vol. MTT-26, pp. 983-987, December 1978.

[13] E. El Hennawy and K. Schunemann, "Computer-aided design of fin-line detectors, modulators and switches," *Arch. Elek. Ubertragung*, vol. 36, pp. 49-56, February 1982.

[14] H. El Hennawy and K. Schunemann. "Hybrid fin-line matching structures." *IEEE Trans. Microwave Theory Tech.*, vol. MTT-30, pp. 2132-2138, December 1982.

[15] H. El Hennawy and K. Schunemann. "Impedance transformation in fin-lines." *IEE Proc. Pt. H. Microwaves Opt. Acoust.*, vol. 129, pp. 342-350, December 1982.

[16] M. Helard, J. Citerne, O. Picon and V. Fouad Hanna, "fin-line." *Electron. Lett.* vol. 19, pp. 537-539, 7th, July 1983.

[17] K. J. Webb and R. Mittra. "Conjugate gradient iterative solution of an integral equation with a small number of Green's function terms: the fin-line discontinuity problem." 1985 North American Radio Science Meeting and International IEEE/AP-S Symposium, Vancouver, Canada.

[18] K. J. Webb and R. Mittra. "Solution of the fin-line step discontinuity problem using the generalized variational technique." *IEEE Trans. Microwave Theory Tech.*, vol. MTT-33, pp. 1004-1010, October 1985.

[19] K. J. Webb and R. Mittra. "A variational solution of the fin-line discontinuity problem." *Proc. European Microwave Conf.*, pp. 311-316, Paris, France, September 1985.

[20] K. J. Webb and R. Mittra. "Numerical solution of planar integrated circuit discontinuities with unknowns in the plane of the metallization." 1986 International IEEE AP-S/URSI Symposium, Philadelphia, PA.

[21] P. Pramanick and P. Bhartia. "Analysis and synthesis of tapered finlines." 1984 IEEE MTT-S International Microwave Symposium Digest, pp. 336-338.

[22] J. H. C. van Heuven. "A new integrated waveguide-microstrip transition." *IEEE Trans. Microwave Theory Tech.*, pp. 144-147, March 1976.

[23] L. J. Lavedan. "Design of waveguide-to-microstrip transitions specially suited to millimeter-wave applications." *Elect. Lett.*, vol. 13, pp. 604-605, September 1977.

[24] L. T. Yuan and P. G. Asher. "A w-band balanced mixer." 1985 IEEE MTT-S International Microwave Symposium Digest, pp. 113-115.

[25] S. J. Nightingale et. al., "A 30 GHz monolithic single balanced mixer with integrated dipole receiving element." 1985 IEEE MTT-S International Microwave Symposium Digest, pp. 116-117.

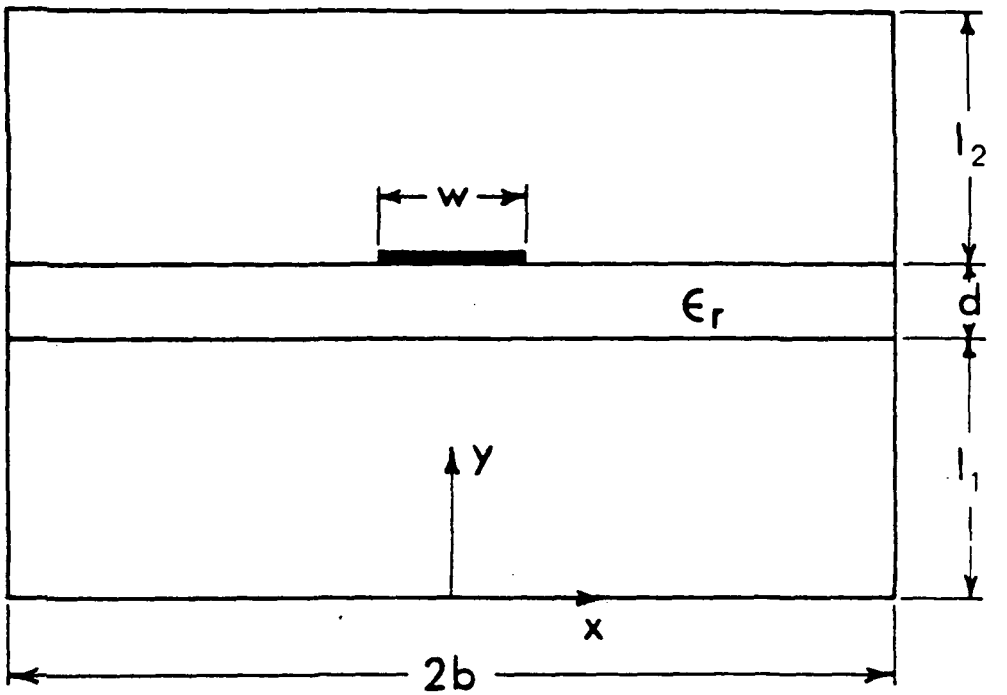

Figure 1. Shielded suspended microstrip.

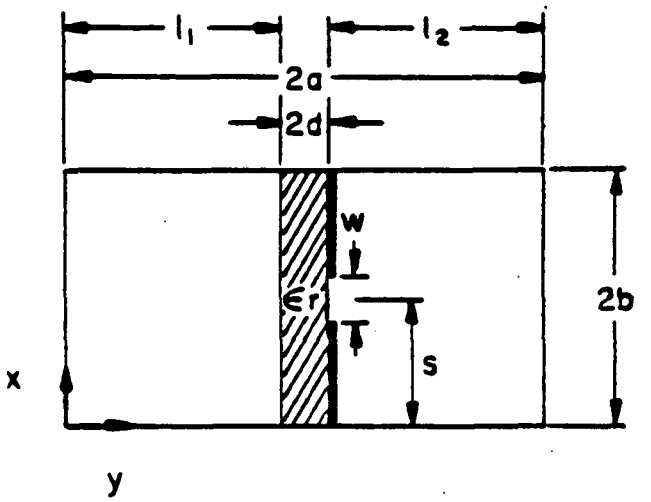

Figure 2. Unilateral finline.

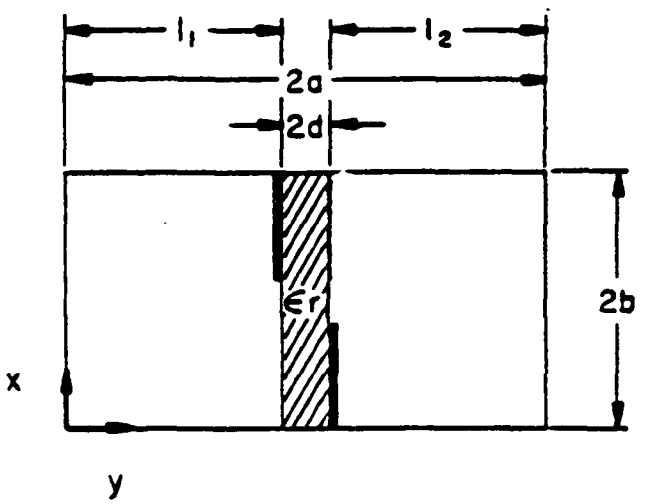

Figure 3. Antipodal finline.

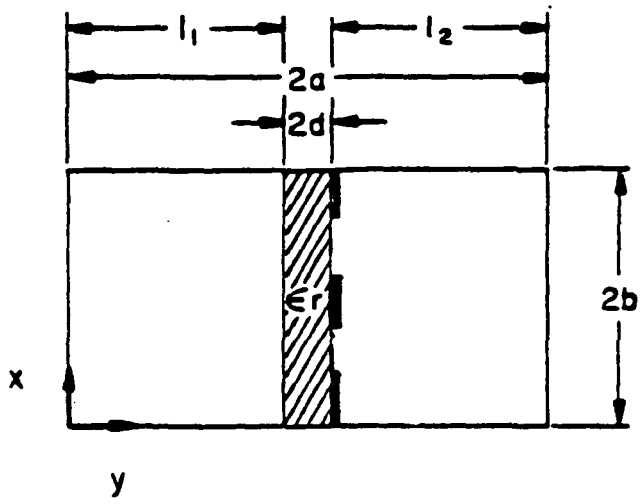

Figure 4. Shielded coplanar waveguide.

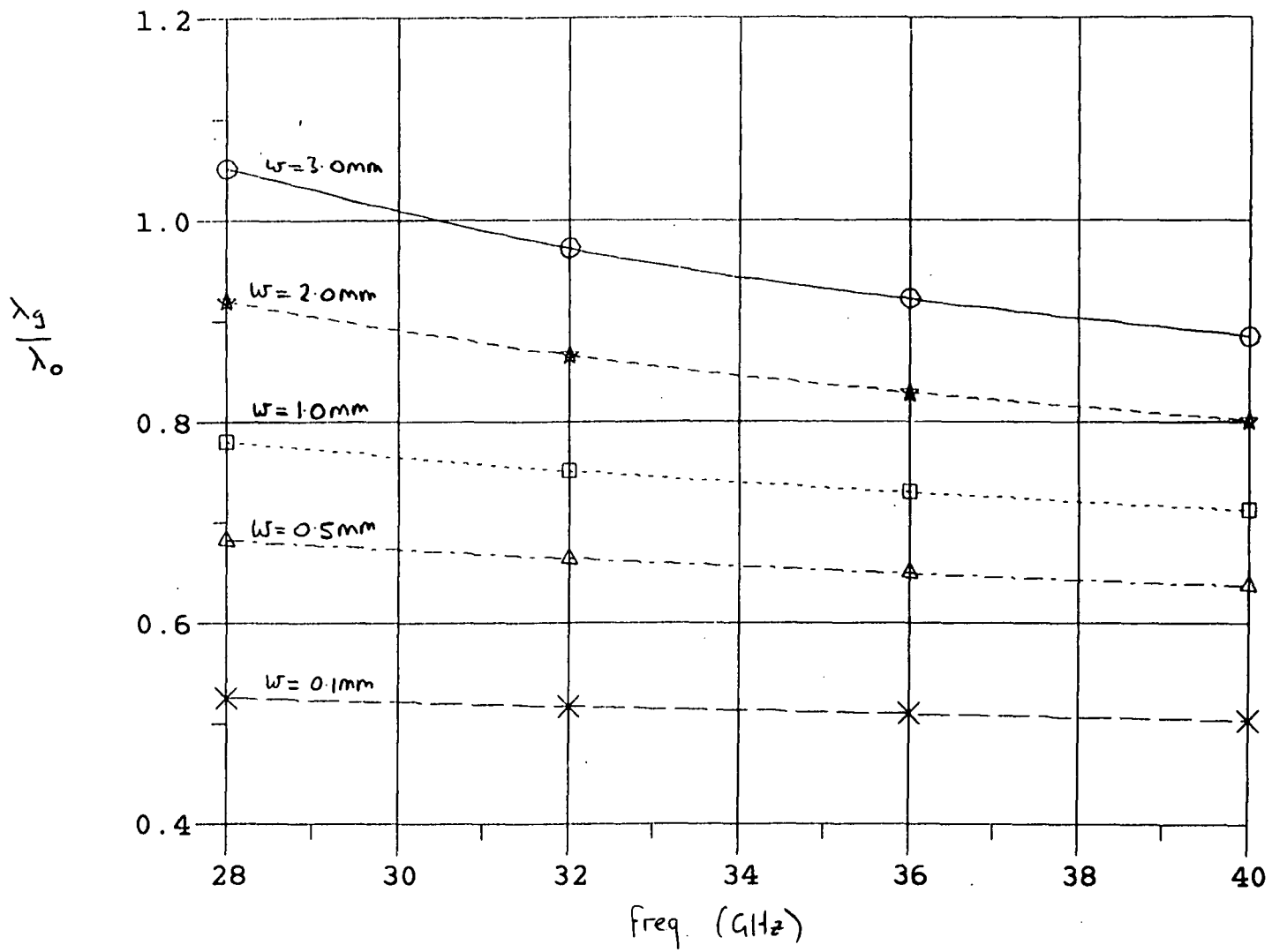

Figure 5. Phase constant curves for the propagating mode in unilateral fin-line with a WR-28 waveguide shield. l_1 = 3.505 mm, l_2 = 3.505 mm, 2d = 0.1 mm, ϵ_r = 13.1, 2b = 3.56 mm.

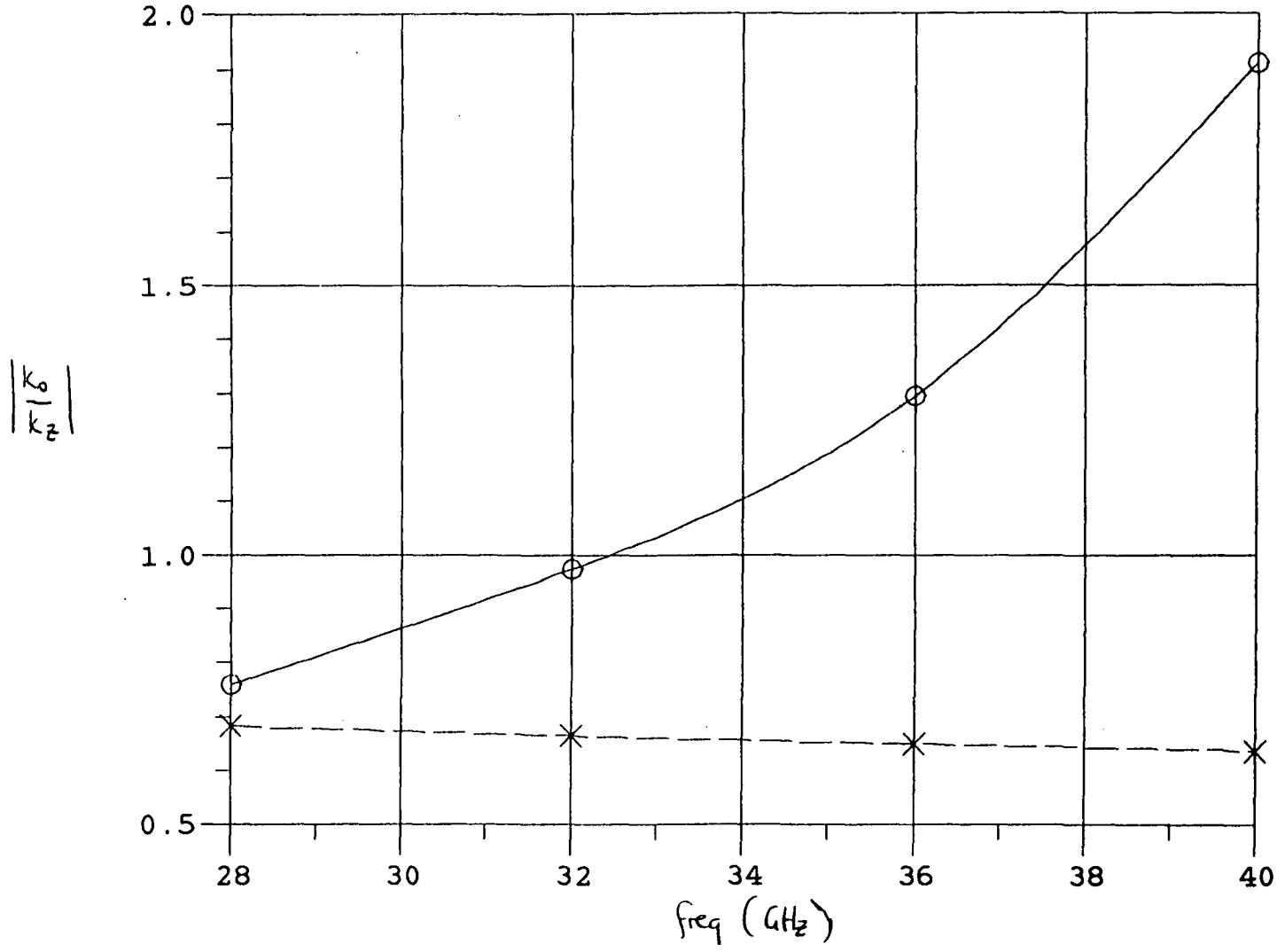

Figure 6. Dispersion curves for two modes (E_x even about x = s) in unilateral fin-line with a WR-28 shield. $l_1 = l_2 = 3.505$ mm, 2d = 0.1 mm, $\epsilon_r = 13.1$, 2b = 3.56 mm, w = 0.5 mm.

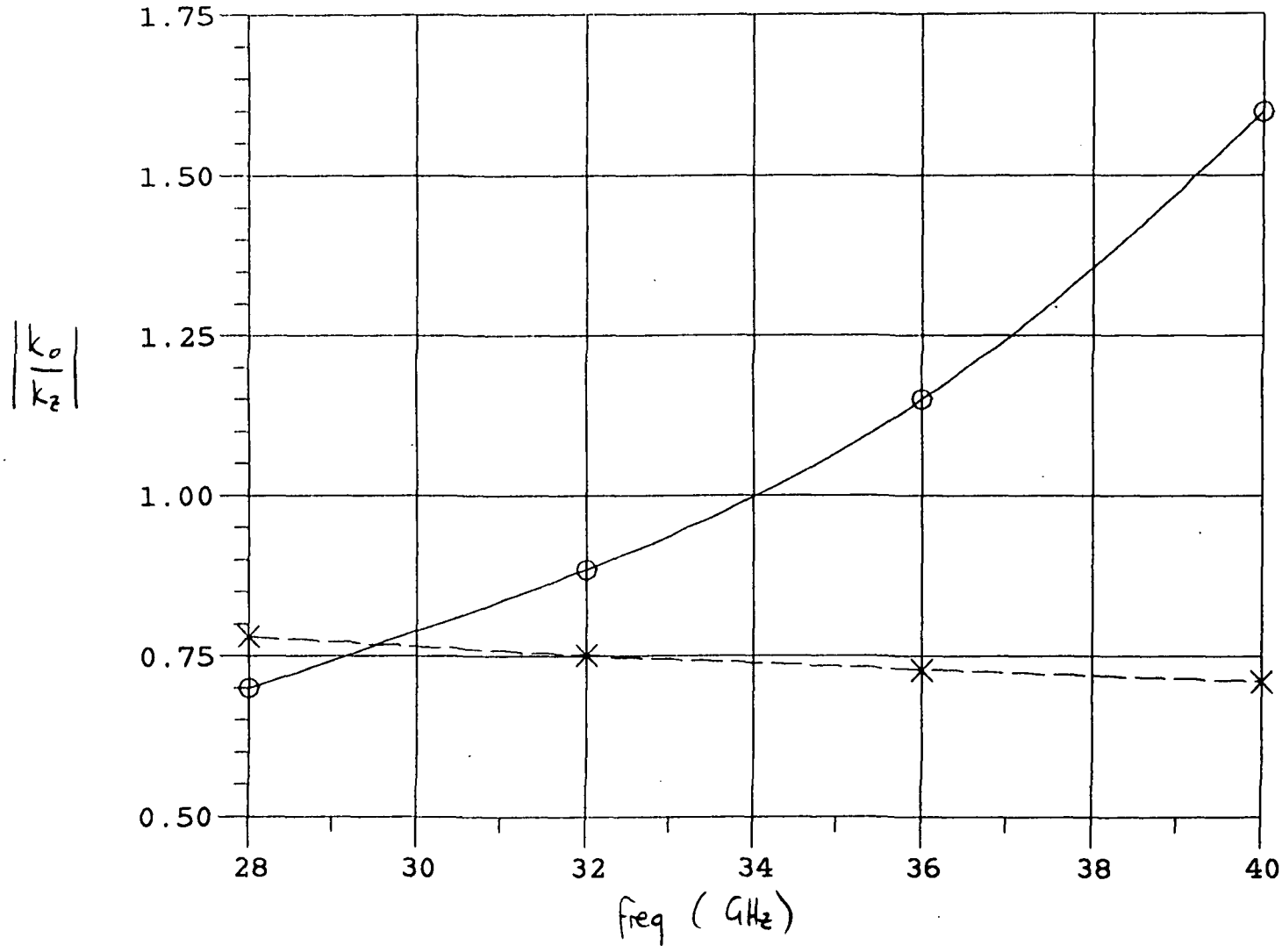

Figure 7. Dispersion curves for two modes (E_x even about x = s) in unilateral fin-line with a WR-28 shield. $l_1 = l_2 = 3505$ mm, 2d = 0.1 mm, $\epsilon_r = 13.1$, 2b = 3.56 mm, w = 1 mm.

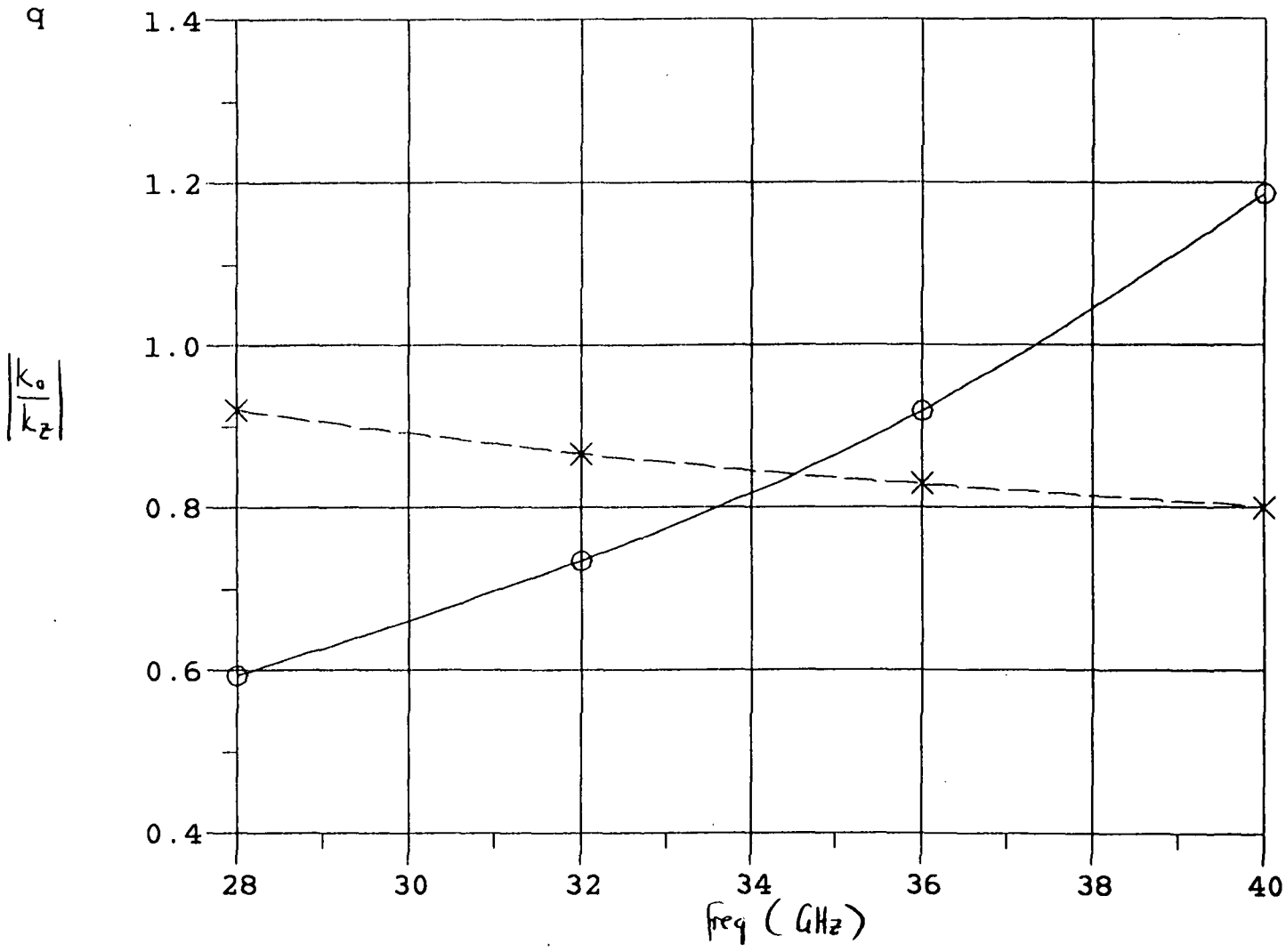

Figure 8. Dispersion curves for two modes (E_x even about x = s) in unilateral fin-line with a WR-28 shield. $l_1 = l_2 = 3.505$ mm, 2d = 0.1 mm, $\epsilon_r = 13.1$, 2b = 3.56 mm, w = 2 mm.

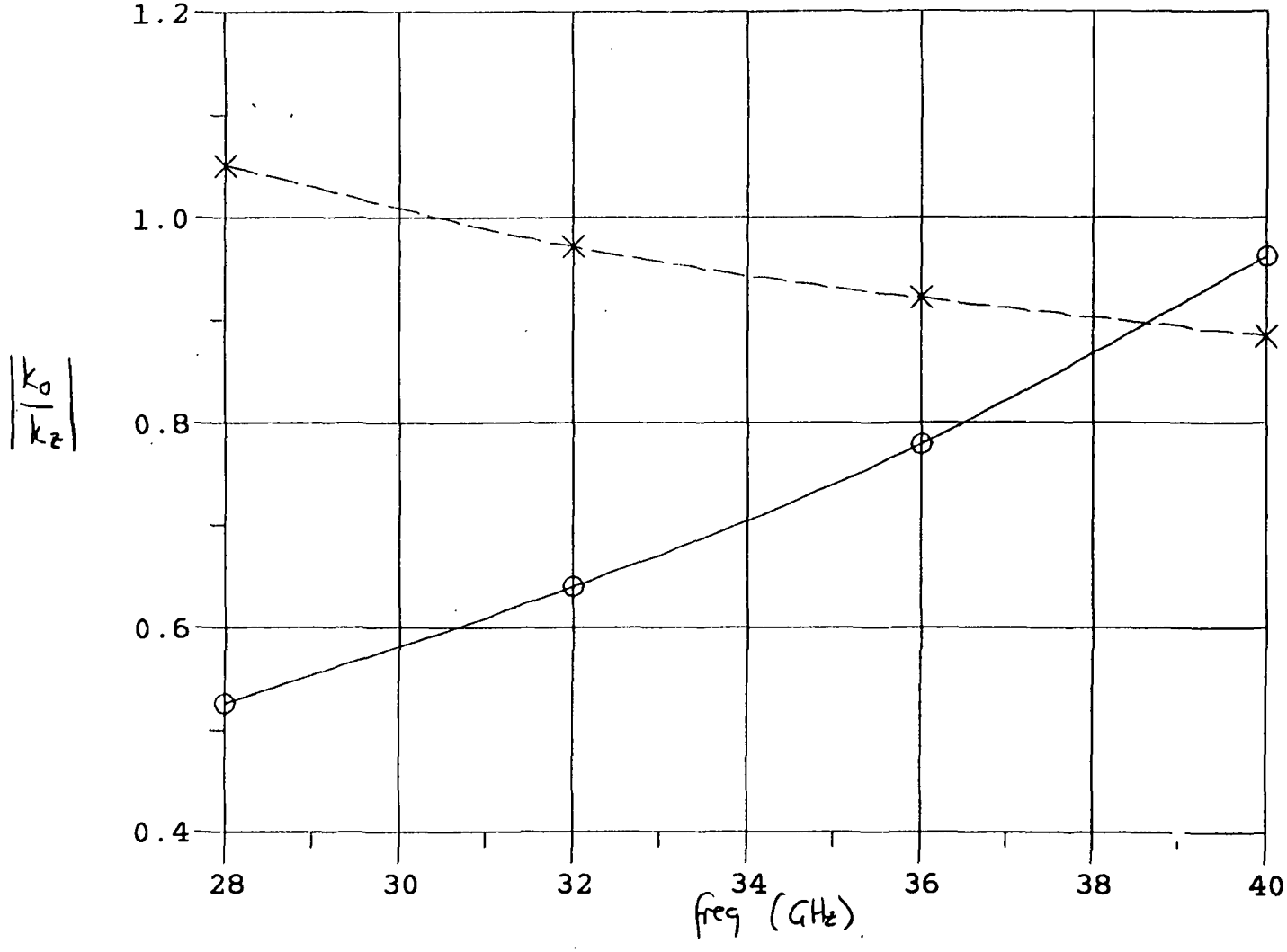

Figure 9. Dispersion curves for two modes (E_x even about x = s) in unilateral fin-line with a WR-28 shield. $l_2 = l_2 = 3.505$ mm, 2d = 0.1 mm, $\epsilon_r = 13.1$, 2b = 3.56 mm, w = 3 mm.

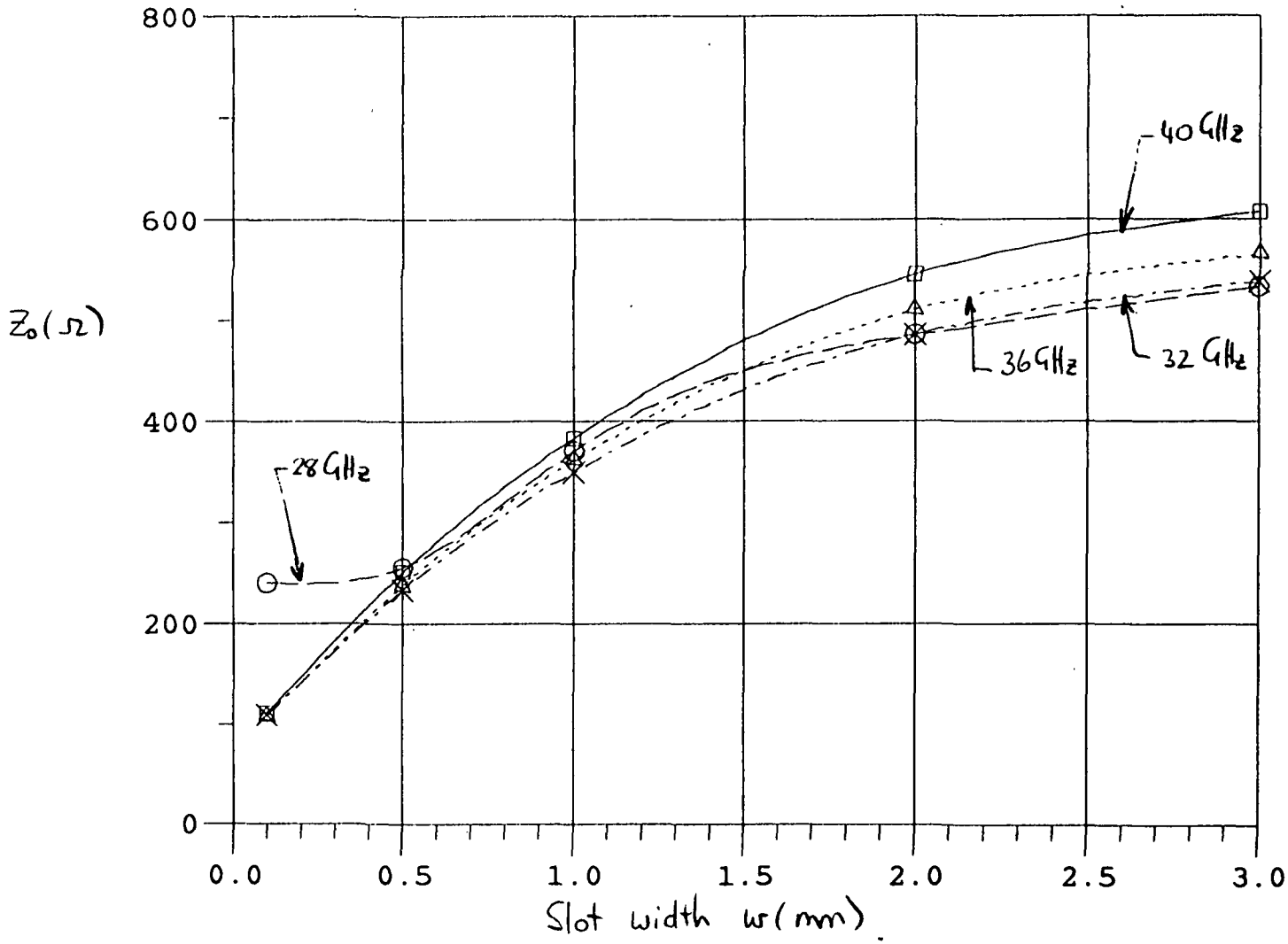

Figure 10. Characteristic impedance for fin-line with a WR-28 shield. $l_1 = l_2 = 3.505$ mm, 2d = 0.1 mm, $\epsilon_r = 13.1$, 2b = 3.56 mm.

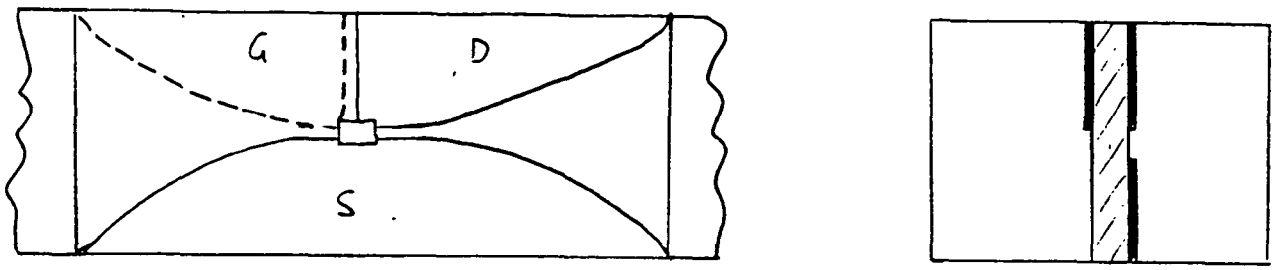

(a)

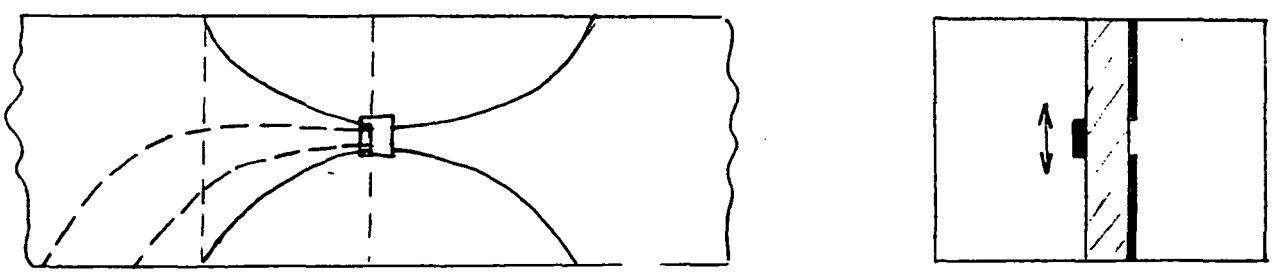

(b)

Figure 11. (a) Unilateral/antipodal finline FET environment. (b) unilateral finline - microstrip FET environment.

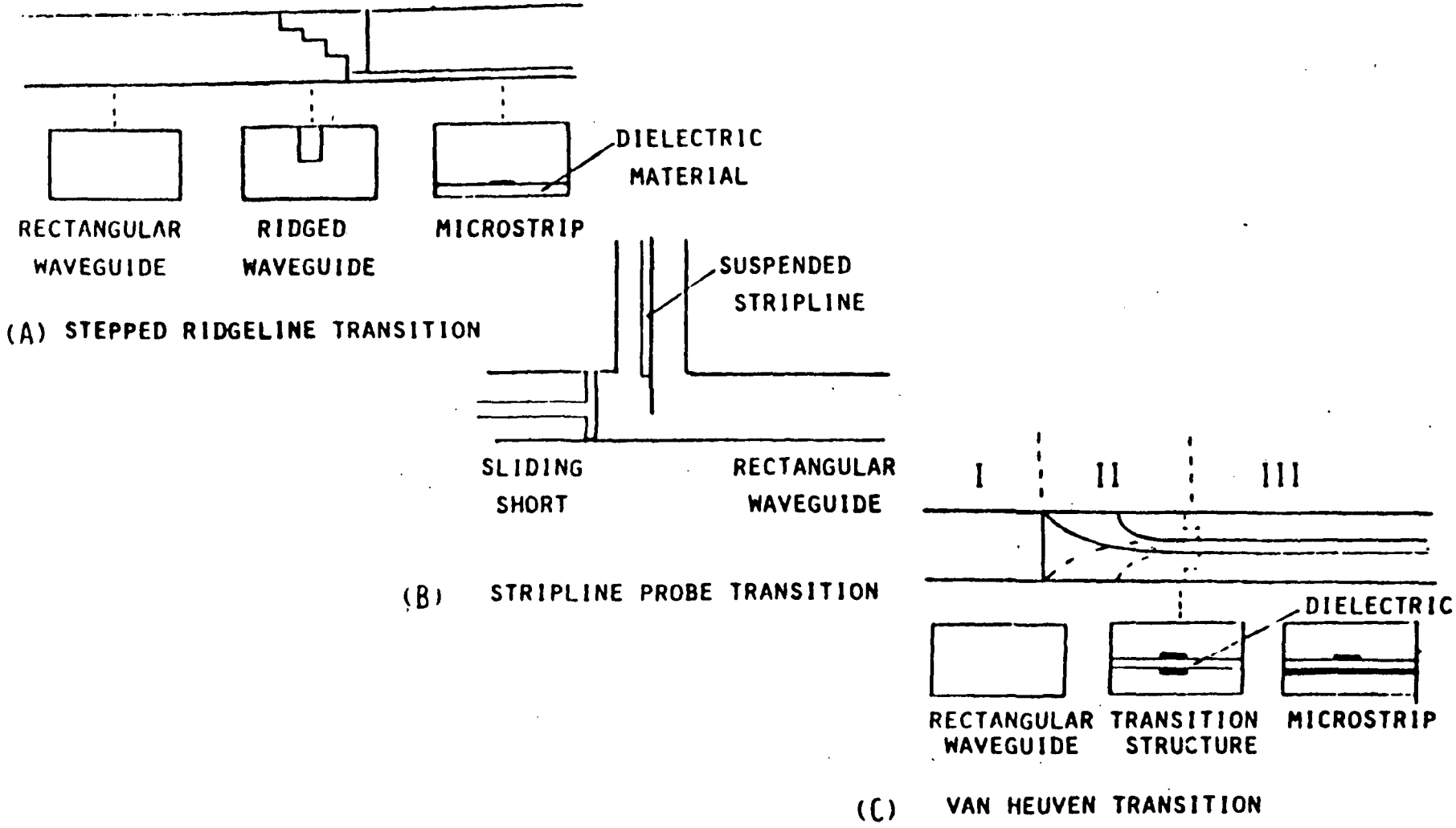

Figure 12. Typical microstrip to waveguide transitions.

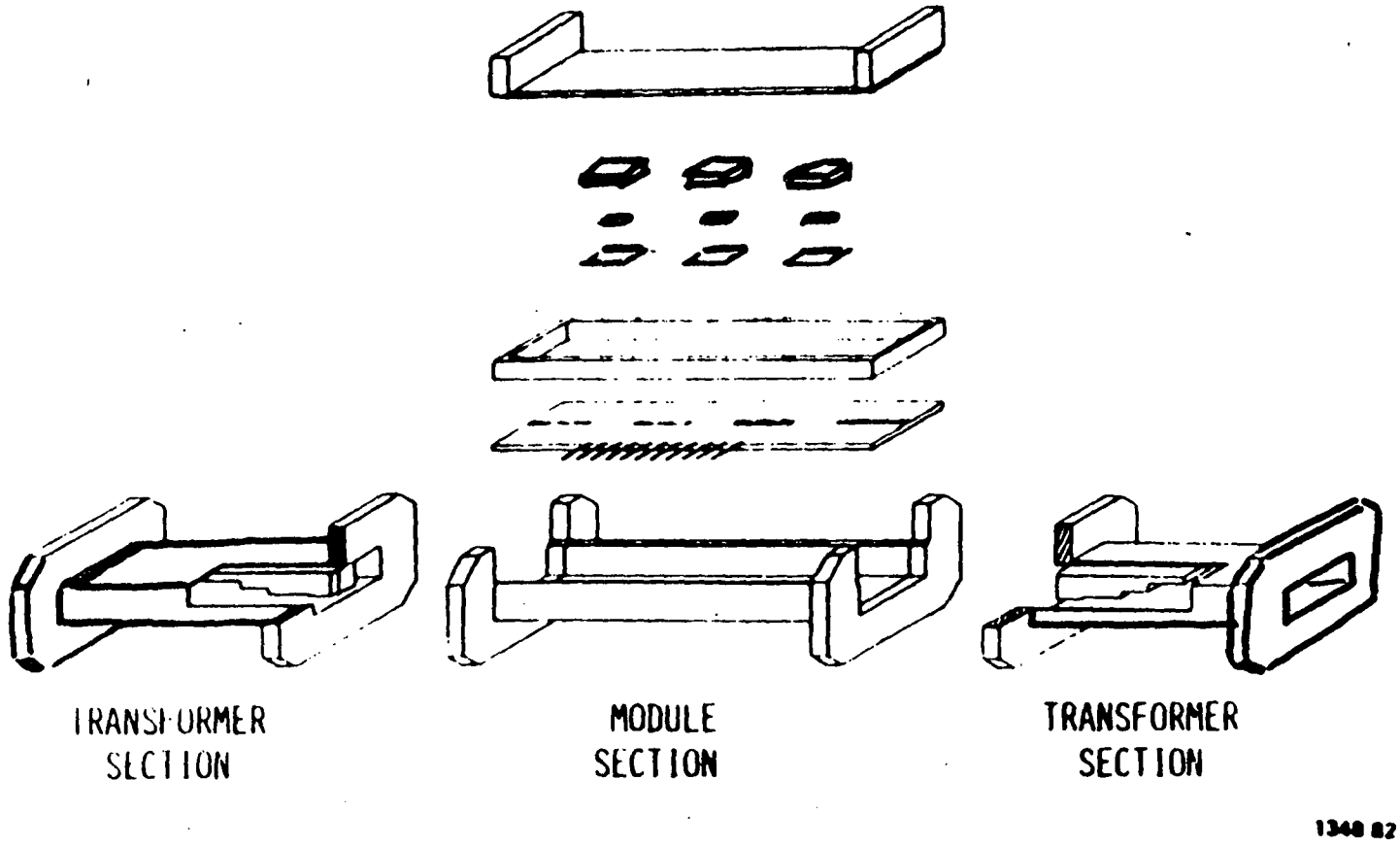

Figure 13. Monolithic module transition and mounting configuration.

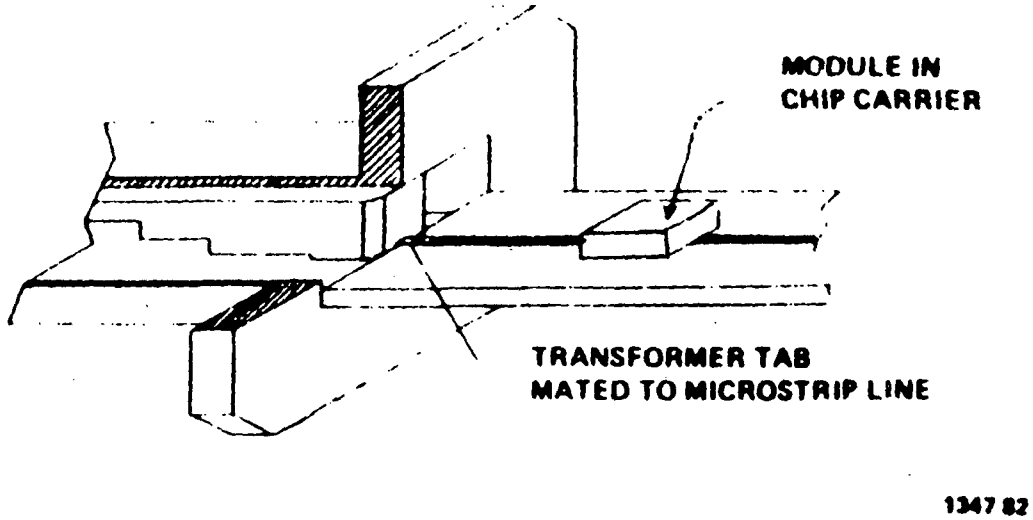

Figure 14. Detail of transformer - microstrip connection.

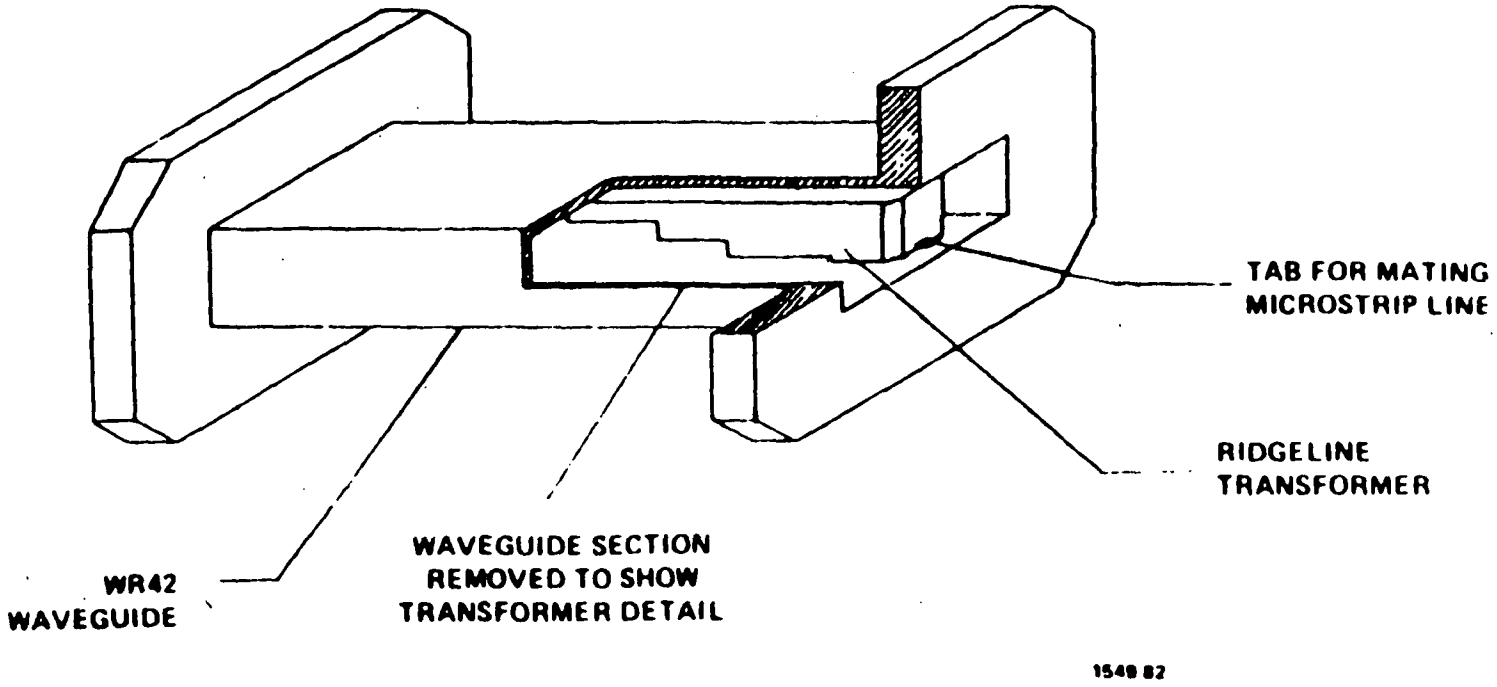

Figure 15. Transformer section.

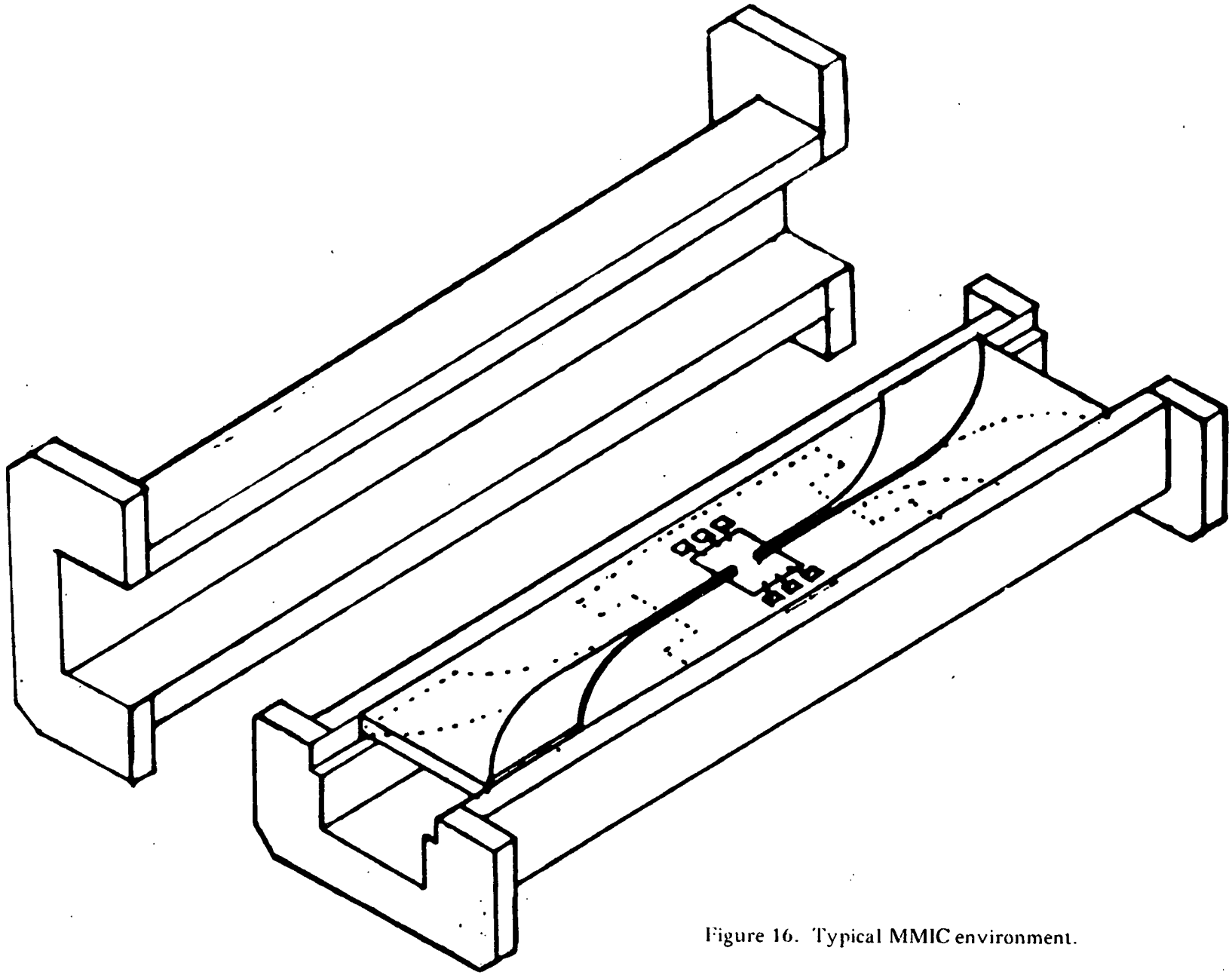

Figure 16. Typical MMIC environment.

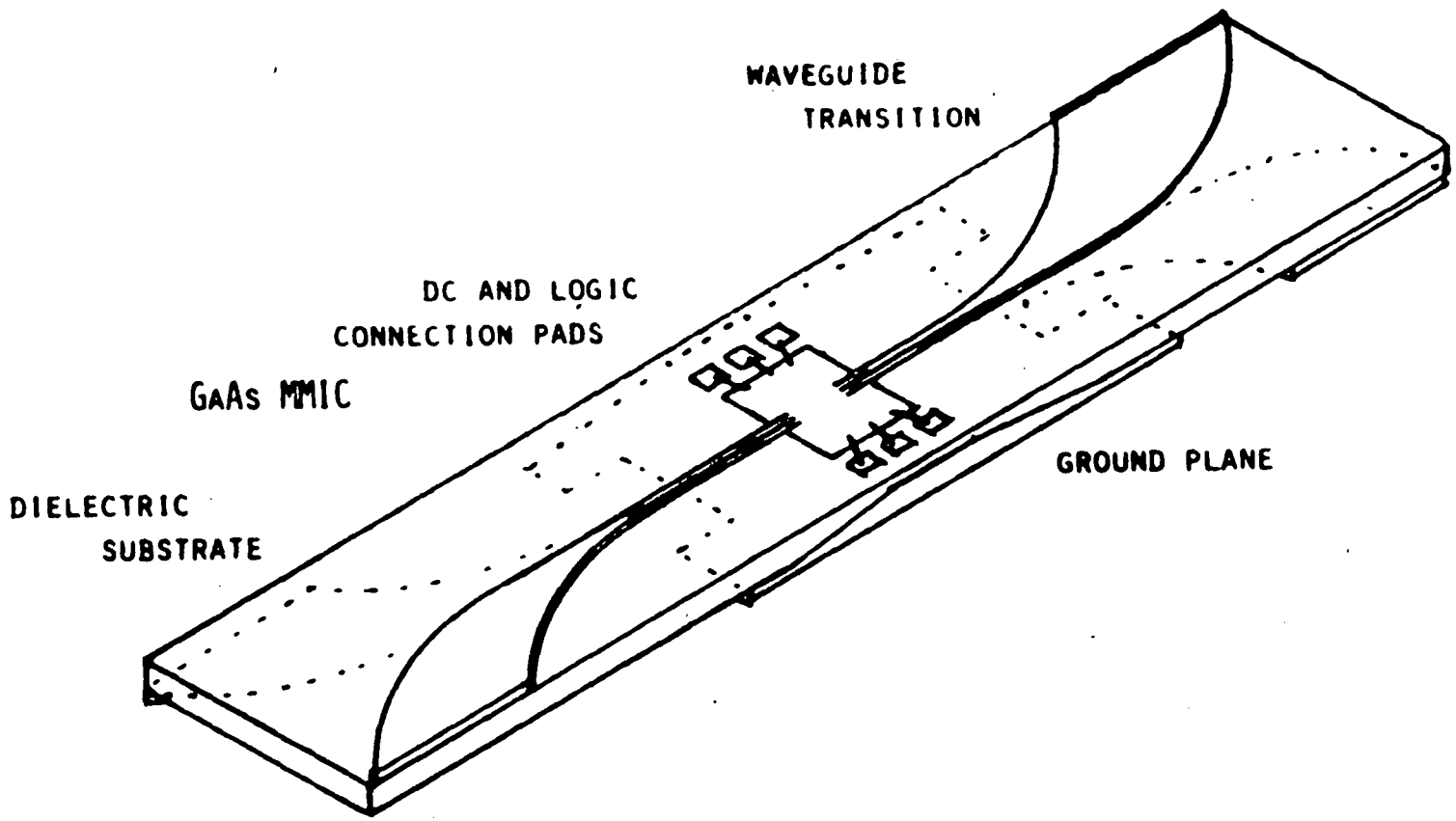

Figure 17. Typical MMIC packaging configuration.

D1
32 P

1823240

N86-30038

Appendix 1

ASYMMETRICAL COUPLED COPLANAR-TYPE TRANSMISSION LINES WITH ANISOTROPIC SUBSTRATES

1B 647432

Toshihide Kitazawa, Yoshio Hayashi and Raj Mittra

ABSTRACT

In this paper the asymmetrical coupled coplanar-type transmission line (C-CTL) with an anisotropic substrate is investigated using both the quasistatic method and the hybrid-mode formulations. The line characteristics of interest, e.g., the propagation constant and the characteristic impedances of the various types of C-CTLs with anisotropic substrate, are presented.

I. INTRODUCTION

Various types of transmission lines with anisotropic substrates have been investigated for use in microwave- and millimeter-wave integrated circuits [1]. These include single and coupled striplines [2] - [7], slot lines [8], and coplanar-type transmission lines [9] - [11]. The coplanar-type transmission lines (CTLs) are promising because of their easy adaptation to shunt element connections [12], [13]. The application of coupled coplanar-type transmission lines to filters and couplers was proposed by C. P. Wen [14]. The propagation characteristics of coupled coplanar-type transmission lines (C-CTL) have been studied based on the quasistatic [14], [15] and hybrid-mode formulations [16], [17], and accurate numerical values are available for the cases with isotropic and/or anisotropic substrates. However, most of them assume the structural symmetry. The theoretical approach for the asymmetrical version is available only for the propagation constant of the case with a single isotropic substrate [16]. There is no information available for the characteristic impedances of asymmetrical C-CTLs, even for the simplest case with an isotropic substrate, although it is required to utilize the advantages of the asymmetrical structure, the impedance transform nature and the additional flexibility.

In this paper, we present the analytical method for the general structure of asymmetrical coupled coplanar-type transmission lines with an anisotropic substrate. This method includes both the hybrid-mode and the quasistatic formulations and is useful for accurately computing the characteristic impedances as well as propagation constants of various types of asymmetrical coupled coplanar-type transmission lines.

II. THEORY

A. Variational Expressions for the Elements of the Capacitance Matrix of a C-CTL

The variational method will be described for the quasistatic characteristics of the general structure for asymmetrical, coupled coplanar-type transmission lines (C-CTLs; Fig. 1) with uniaxially anisotropic substrates, whose permittivities are given by the following dyadic:

$$\varepsilon_i = \begin{bmatrix} \varepsilon_{i,xx} & \varepsilon_{i,xy} \\ \varepsilon_{i,xy} & \varepsilon_{i,yy} \end{bmatrix} \varepsilon_0 \tag{1}$$

The quasistatic characteristics of the symmetrical C-CTL can be expressed in terms of the scalar line capacitance [15], whereas, for the asymmetrical C-CTL case considered here, they are described by the capacitance matrix which is defined as:

$$\begin{bmatrix} Q_1 \\ Q_2 \end{bmatrix} = \begin{bmatrix} C_1 & -C_m \\ -C_m & C_2 \end{bmatrix} \begin{bmatrix} V_1 \\ V_2 \end{bmatrix} \tag{2}$$

where V_1 and Q_1 are the potential and the total charge on the right strip, and V_2 and Q_2 are those on the left strip, respectively. The variational expressions of the self and mutual capacitances C_1, C_2, and C_m will be derived in the following.

The charge distribution on the conductors can be expressed in terms of the aperture field $e_x(x)$ [15];

$$\sigma(x) = \iint_{-\infty}^{\infty} G(\alpha;x|x')\, e_x(x')\, d\alpha\, dx' \tag{3}$$

with

$$G(\alpha;x|x') = -j\,\frac{\alpha}{2}\,F(\alpha)\, e^{j\alpha(x-x')} \tag{4}$$

$$F(\alpha) = \frac{\varepsilon_0}{\pi|\alpha|}\left(Y_U(\alpha) + Y_L(\alpha)\right) \tag{5}$$

where Y_U and Y_L can be obtained by utilizing the simple recurrent relation (Appendix). The total charge located between x_1 and x_2 is given by

$$Q(x_1,x_2) = \int_{x_2}^{x_1} \sigma(x)\, dx \tag{6}$$

When x_1 and x_2 lie in slots, $Q(x_1,x_2)$ should be constant, that is,

$$\begin{aligned} Q(x_1,x_2) &= Q_1(|x_2| < a \text{ and } b_1 < x_1 < c_1) \\ &= Q_2(-c_2 < x_2 < -b_2 \text{ and } |x_1| < a) \end{aligned} \tag{7}$$

We consider the following sets of excitations to determine the capacitances:

i) $V_1 \neq 0, \quad V_2 = 0$ (8a)

ii) $V_1 = 0, \quad V_2 \neq 0$ (8b)

iii) $V_1 = -V_2$ (8c)

Multiplying (6) by $e_x(x_1)$ and integrating over the right slot ($b_1 < x_1 < c_1$), we obtain

$$Q_1V_1 = \int_{b_1}^{c_1} e_x(x_1)\, Q(x_1,x_2)\, dx_1$$

$$= \frac{1}{2} \iint_{-\infty}^{\infty} F(\alpha)\, e_x(x')\, e^{j\alpha x'} \left\{\int_{b_1}^{c_1} e_x(x_1)\, e^{-j\alpha x_1}\, dx_1 - V_1\, e^{-j\alpha x_2}\right\} d\alpha\, dx'$$

$$(|x_2| < a) \tag{9}$$

by utilizing

$$V_1 = \int_{b_1}^{c_1} e_x(x)\, dx = -\int_{-a}^{a} e_x(x)\, dx \tag{10}$$

Then, multiplying Eq. (9) by $e_x(x_2)$ and integrating over the left slot, we obtain

$$-Q_1V_1^2 = \iint e_x(x_1)\, Q(x_1,x_2)\, e_x(x_2)\, dx_1\, dx_2$$

$$= \frac{1}{2} \iint_{-\infty}^{\infty} F(\alpha)\, e_x(x')\, e^{j\alpha x'} \left\{-V_1 \int_{b_1}^{c_1} e_x(x_1)\, e^{-j\alpha x_1}\, dx_1\right.$$

$$\left. - V_1 \int_{-c_2}^{-b_2} e_x(x_2)\, e^{-j\alpha x_2}\, dx_2\right\} d\alpha\, dx' \tag{11}$$

That is,

$$Q_1V_1 = \int_0^{\infty} \iint_{-\infty}^{\infty} F(\alpha)\, e_x(x')\, \cos\alpha(x - x')\, e_x(x)\, dx'\, dx\, d\alpha \tag{12}$$

Therefore, we obtain the stationary expression of C_1 as follows:

$$C_1 = \left.\frac{Q_1}{V_1}\right|_{V_2 = 0}$$

$$= \frac{\iint_{-\infty}^{\infty} \int_0^{\infty} e_x(x)\ F(\alpha)\ \cos\ \alpha(x - x')\ e_x(x')\ d\alpha\ dx'dx}{\{\int e_x(x)\ dx\}^2} \tag{13}$$

Equation (13) gives an upper bound to the exact value. Similar expressions for C_2 and $C_1 + 2C_m + C_2$ can be obtained by using (8b) and (8c), respectively. The Ritz procedure will be applied to the variational expressions (13) for the numerical computation.

There are two fundamental modes of propagation in asymmetrical coupled coplanar-type transmission lines (C-CTL), that is, c- and π-modes, which become even and odd modes in the symmetrical case, respectively. The propagation characteristics of an asymmetrical C-CTL can be expressed in terms of two propagation constants, β_c, β_π, and four characteristic impedances, $Z_{i,c}$, $Z_{i,\pi}$ (i = 1,2), where i = 1 and 2 stand for the right and left strips, respectively. The quasistatic values of the propagation constants and the characteristic impedances for two fundamental modes can be calculated by [6], [18]

$$\beta_{c,\pi} = \frac{\omega}{\sqrt{2}} \{L_1C_1 + L_2C_2 - 2L_mC_m \pm U\}^2$$

$$Z_{1,c} = \frac{\omega}{\beta_c} (L_1 - L_m/R_\pi)$$

$$Z_{1,\pi} = \frac{\omega}{\beta_\pi}(L_1 - L_m/R_c)$$

$$Z_{2,c} = -R_c R_\pi Z_{1,c}$$

$$Z_{2,\pi} = -R_c R_\pi Z_{1,\pi}$$

$$R_{c,\pi} = \frac{L_2C_2 - L_1C_1 \pm U}{2(L_mC_2 - L_1C_m)}$$

$$U = \left\{(L_2C_2 - L_1C_1)^2 + 4(L_mC_1 - L_2C_m)(L_mC_2 - L_1C_m)\right\}^{1/2} \tag{14}$$

where L_1, L_2, and L_m are the self and mutual inductances, which can be obtained from C_1, C_2, and C_m for the case without a substrate.

B. Hybrid-mode Analysis

The network analytical method of electromagnetic fields has been successfully applied to analyze the propagation characteristics of various types of planar transmission lines with isotropic and/or uniaxially anisotropic substrates whose optical axis is coincident with one of the coordinate axes [5], [9], [10]. This method is based on the hybrid-mode formulation, and no approximations for simplication are used in the formulation procedure. The propagation constants of an asymmetrical C-CTL can be obtained easily by using the extended version of this method and applying the Galerkin's procedure. The characteristic impedance is not uniquely specified because of the hybrid mode of propagation. The definition chosen here is

$$Z_{i,j} = \frac{V_{i,j}}{I_{i,j}} \qquad (i = 1,2; \quad j = c,\pi) \tag{15}$$

where $I_{1,j}$ and $V_{1,j}$ are the total current on the right strip and the voltage difference between the right strip and the ground conductor, respectively, and $I_{2,j}$ and $V_{2,j}$ are those for the left strip. The frequency-dependent hybrid-mode solutions for propagation constants and characteristic impedances are presented in Section III.

C. Coplanar-type Transmission Line

The quasistatic and hybrid-mode formulations described above are quite general and applicable to various configurations, e.g., coupled coplanar waveguide (C-CPW; Fig. 2(a)), coupled CPW with double-layered substrate (Fig. 2(b)), coupled sandwich CPW (Fig. 2(c)) and coupled coplanar three strips (Fig. 2(d)). In the coplanar-strip case of Fig. 2(d), the charge and current distribution on the strips are the basic quantities as opposed to the aperture fields in the CPW cases of Figs. 2(a) - (c). Numerical results for these coplanar-type transmission lines are included in the next section.

III. NUMERICAL EXAMPLES

Figure 3 shows the quasistatic characteristics of an asymmetrical coupled coplanar waveguide with an isotropic substrate. Figures 3(a) and (b) depict the effective dielectric constants $\varepsilon_{eff,j}$ and the characteristic impedances $Z_{i,j}(j = c,\pi)$ as a function of the strip width ratio S_{2/S_1}. $\varepsilon_{eff,j}$ is obtained by

$$\varepsilon_{eff,j} = (\beta j/\omega\sqrt{\varepsilon_0\mu_0})^2 \tag{16}$$

The values for the symmetrical case($S_{2/S_1} = 1$) are in good agreement with those of [15]. Another check on the results can be made by investigating the limiting case as S_{2/S_1} becomes very large, where the left slot is decoupled and $\varepsilon_{eff,\pi}$ converges to that of the asymmetrical coplanar waveguide (ACPW)[15] shown in Fig. 4(a). As S_{2/S_1} becomes very small, $\varepsilon_{eff,c}$ converges to that of ACPW shown in Fig. 4(b), which can be considered as the limiting case of $S_{2/S_1} = 0$. Figures 5 and 6 show the quasistatic characteristics of asymmetrical coupled double-layered (Fig. 2(b)) and sandwich (Fig. 2(c)) coplanar waveguides, respectively. They depict $\varepsilon_{eff,j}$ and $Z_{i,j}(j = c,\pi)$ as functions of the ratio of the thickness of the upper to the lower layer d/h. Figure 7 shows the frequency dependence of the effective dielectric constants for various types of a coupled coplanar waveguide with uniaxially anisotropic substrates cut with their planar surface perpendicular to the optical axis. The frequency-dependent hybrid-mode values of each mode converge precisely to the corresponding quasistatic values in lower frequency ranges for all cases. The phase velocities of two fundamental modes of the case with double-layered substrates have close values in the higher-frequency range, but they never coincide because of the mode coupling.

The mode of propagation can not be identified as the c- or π-mode by investigating the voltage and current. Figure 8 shows the frequency dependence of the characteristic impedances of a coupled coplanar waveguide. Figure 9 shows the effective dielectric constants and the characteristic impedances of coupled coplanar three strips (Fig. 2(d)) with a uniaxially anisotropic substrate. The definition for the characteristic impedance of coupled coplanar strips is chosen as

$$Z_{i,j} = \frac{V_{i,j}}{I_{i,j}} \tag{17}$$

where $I_{1,j}$ and $V_{1,j}$ are the total current on the right strip and the voltage between the right and the center strips, and $I_{2,j}$ and $V_{2,j}$ are those for the left strip. Again, the frequency-dependent values converge to the quasistatic values in the lower-frequency ranges.

Figure 10 shows $\varepsilon_{eff,i}$ and $Z_{i,j}$ of an asymmetrical coupled coplanar waveguide on a uniaxially anisotropic substrate cut with its surface at γ to the optical axis.

V. CONCLUSIONS

This paper describes the analytical method for the general structure of asymmetrical coupled coplanar-type transmission lines (C-CTLs) with anisotropic media. It consists of the quasistatic and the hybrid-mode formulations. The former gives variational expressions for the line parameters of the cases with the uniaxially anisotropic substrate cut with its planar surface at an arbitrary angle to the optical axis; the latter gives the rigorous frequency-dependent characteristics for the cases with the anisotropic substrate cut with its surface perpendicular to the optical axis. Some numerical examples showed the accuracy of the method and presented the propagation characteristics, the propagation constants as well as the characteristic impedances of the various types of C-CTL with anisotropic media, for the first time.

APPENDIX: RECURRENT RELATIONS

The Fourier transform of the electric field E_x and the electric flux density D_y in the layer $i(y_{i+1} > y > y_i)$ can be expressed as:

$$\tilde{E}_x(\alpha;x) = \frac{1}{\sqrt{2\pi}} \int_{-\infty}^{\infty} E_x(x,y)\, e^{-j\alpha x}\, dx$$

$$= \exp(-b_i y)[A_i \cosh(p_i y) + B_i \sinh(p_i y)] \tag{A1}$$

$$\tilde{D}_y(\alpha;x) = \varepsilon_{i,xy}\, \varepsilon_0\, \tilde{E}_x + \varepsilon_{i,yy}\varepsilon_0\, \tilde{E}_y$$

$$= -\varepsilon_{i,yy}\varepsilon_0\, p_i\, \exp(-b_i y)[A_i \sinh(p_i y) + B_i \cosh(p_i y)] \tag{A2}$$

where A_i, B_i are unknown constants and

$$b_i = j\, \frac{\varepsilon_{i,xy}}{\varepsilon_{i,yy}}\, \alpha \tag{A3}$$

$$p_i = \frac{\varepsilon_{i,e}}{\varepsilon_{i,yy}}\, |\alpha| \tag{A4}$$

$$\varepsilon_{i,e} = \sqrt{\varepsilon_{i,xx}\, \varepsilon_{i,yy} - \varepsilon_{i,xy}^2} \tag{A5}$$

We will derive the recurrent relation in the upper region $y > 0$. Define the following quantity at the lower surface of the layer i (Fig. 11):

$$Y_i = \frac{j\alpha}{\varepsilon_{i,e}\varepsilon_0|\alpha|} \cdot \left.\frac{\tilde{D}_y}{\tilde{E}_x}\right|_{y=y_i+0} \tag{A6}$$

Considering the continuity conditions at the $y = y_{i+1}$ plane, we obtain the following recurrent relation with respect to Y_i

$$Y_i = \frac{\frac{\varepsilon_{i+1,e}}{\varepsilon_{i,e}} Y_{i+1} - \tanh(p_i d_i)}{1 = \frac{\varepsilon_{i+1,e}}{\varepsilon_{i,e}} Y_{i+1} \tanh(p_i d_i)} \tag{A7}$$

The electric flux density at the $y = +0$ plane (the slot plane) can be obtained as

$$\tilde{D}_y(\alpha; y = +0) = \frac{\varepsilon_{N,e}\varepsilon_0|\alpha|}{j\alpha} Y_N \tilde{e}_x \tag{A8}$$

where $\tilde{e}_x$ is the Fourier transform of the aperture field $e_x(x)$. Then, Y_U in Eq. (5) can be obtained as

$$Y_u = \varepsilon_{N,e} Y_N \tag{A9}$$

A similar recurrent relation holds in the lower region $y < 0$, and Y_L can be determined.

REFERENCES

[1] N. G. Alexopoulos, "Integrated-circuit structures on anisotropic substrates," IEEE Trans. Microwave Theory Tech., vol. MTT-33, pp. 847-881, Oct. 1985.

[2] N. G. Alexopoulos, C. M. Krowne, and S. Kerner, "Dispersionless coupled microstrip over fused silica-like anisotropic substrates," Electron. Lett., vol. 12, pp. 579-580, Oct. 1976.

[3] N. G. Alexopoulos and C. M. Krowne, "Characteristics of single and coupled microstrips on anisotropic substrates," IEEE Trans. Microwave Theory Tech., vol. MTT-26, pp. 387-393, June 1978.

[4] M. Kobayashi and R. Terakado, "Method for equalizing phase velocities of coupled microstrip lines by using anisotropic substrate," IEEE Trans. Microwave Theory Tech., vol. MTT-28, pp. 719-722, July 1980.

[5] T. Kitazawa and Y. Hayashi, "Propagation characteristics of striplines with multilayered anisotropic media," IEEE Trans. Microwave Theory Tech., vol. MTT-31, pp. 429-433, June 1983.

[6] T. Kitazawa and R. Mittra, "Analysis of asymmetric coupled striplines," IEEE Trans. Microwave Theory Tech., vol. MTT-33, pp. 643-646, July 1985.

[7] T. Kitazawa, Y. Hayashi, K. Fujita, and H. Mukaihara, "Analysis of broadside-coupled strip lines with anisotropic substrate," Trans. IECE Japan, vol. 66-B, no. 9, pp. 1139-1146, Sept. 1983.

[8] Y. Hayashi, T. Kitazawa and M. Suzuki, "Dispersion characteristic of slot line on a sapphire substrate," Trans. IECE Japan, vol. 63-B, no. 10, pp. 1013-1014, Oct. 1980.

[9] Y. Hayashi, T. Kitazawa and S. Sasaki, "Analysis of coplanar strip lines on an anisotropic substrate using Galerkin's method," Trans. IECE Japan, vol. 64-B, no. 7, pp. 666-673, July 1981.

[10] T. Kitazawa and Y. Hayashi, "Coupled slots on an anisotropic sapphire substrate," IEEE Trans. Microwave Theory Tech., vol. MTT-29, pp. 1035-1040, Oct. 1981.

[11] T. Kitazawa and Y. Hayashi, "Quasi-static characteristics of coplanar waveguide on a sapphire substrate with its optical axis inclined," IEEE Trans. Microwave Theory Tech., vol. MTT-30, pp. 920-922, Oct. 1982.

[12] C. P. Wen, "Coplanar waveguide: A surface strip transmission line suitable for nonreciprocal gyromagnetic device applications," IEEE Trans. Microwave Theory Tech., vol. MTT-17, pp. 1087-1090, Dec. 1969.

[13] J. B. Knorr and K. D. Kuchler, "Analysis of coupled slots and coplanar strips on dielectric substrate," IEEE Trans. Microwave Theory Tech., vol. MTT-23, pp. 541-548, July 1975.

[14] C. P. Wen, "Coplanar-waveguide directional couplers," IEEE Trans. Microwave Theory Tech., vol. MTT-18, pp. 318-322, June 1970.

[15] T. Kitazawa and R. Mittra, "Quasistatic characteristics of asymmetrical and coupled coplanar-type transmission lines," IEEE Trans. Microwave Theory Tech., vol. MTT-33, pp. 771-778, Sept. 1985.

[16] B. J. Janiczak, "Behaviour of guided modes in systems of parallelly located transmission lines on dielectric substrates," Electron. Lett., vol. 19, pp. 778-779, Sept. 1983.

[17] T. Kitazawa and Y. Hayashi, "Coupled coplanar waveguide with anisotropic substrate," to be published.

[18] T. Kitazawa and Y. Hayashi, "Analysis of unsymmetrical broadside-coupled striplines with anisotropic substrates," to be published.

LIST OF ILLUSTRATIONS

Fig. 1. General structure of asymmetrical coupled coplanar-type transmission lines with anisotropic substrates.

Fig. 2. (a) Asymmetrical coupled coplanar waveguide (C-CPW).

Fig. 2. (b) Asymmetrical coupled coplanar waveguide with double-layered substrate.

Fig. 2. (c) Asymmetrical coupled sandwich coplanar waveguide.

Fig. 2. (d) Asymmetrical coupled coplanar three strips.

Fig. 3. Quasistatic characteristics of asymmetrical coupled coplanar waveguide versus strip-width ratio S_{2/S_1}.

(a) Effective dielectric constants
(b) Characteristic impedances

$\varepsilon_{1xx} = \varepsilon_{1yy} = 9.6$, $\varepsilon_{1xy} = 0$

$2a/h = 1$, $S_{1/h} = 2$, $W_{1/h} = 2$, $W_{2/h} = 2$.

Fig. 4. Asymmetrical coplanar waveguide (ACPW).

Fig. 5. Quasistatic characteristics of asymmetrical coupled coplanar waveguide with double-layered substrate.

$\varepsilon_{1xx} = 9.4$, $\varepsilon_{1yy} = 11.6$, $\varepsilon_{2xx} = \varepsilon_{2yy} = 2.6$, $\varepsilon_{ixy} = 0$ $(i = 1,2)$

$S_{1/h} = 1.0$, $S_{2/h} = 0.5$, $W_{1/h} = 1.5$, $W_{2h} = 2.0$.

Fig. 6. Quasistatic characteristics of asymmetrical coupled sandwich coplanar waveguide.

$\varepsilon_{1xx} = \varepsilon_{2xx} = 9.4$, $\varepsilon_{1yy} = \varepsilon_{2yy} = 11.6$, $\varepsilon_{ixy} = 0$ $(i = 1,2)$

$S_{1/h} = 1.0$, $S_{2/h} = 0.5$, $W_{1/h} = 1.5$, $W_{2/h} = 2.0$.

Fig. 7. Dispersion characteristics of various types of coupled coplanar waveguides.

$S_{1/h} = 1.0$, $S_{2/h} = 0.5$, $W_{1/h} = 1.5$, $W_{2/h} = 2.0$

(a) Asymmetrical coupled coplanar waveguide (C-CPW).

$\varepsilon_{1xx} = 9.4$, $\varepsilon_{1yy} = 11.6$, $\varepsilon_{1xy} = 0$.

(b) Asymmetrical coupled coplanar waveguide with double-layered substrate.

$\varepsilon_{1xx} = 9.4$, $\varepsilon_{1yy} = 11.6$, $\varepsilon_{2xx} = \varepsilon_{2yy} = 2.6$,

$\varepsilon_{ixy} = 0$ $(i = 1,2)$, $d/h = 0.1$.

(c) Asymmetrical coupled sandwich coplanar waveguide.

$\varepsilon_{1xx} = \varepsilon_{2xx} = 9.4$, $\varepsilon_{1yy} = \varepsilon_{2yy} = 11.6$,

$\varepsilon_{ixy} = 0$ $(i = 1,2)$, $d/h = 1.0$.

———— : Hybrid-mode, ——— - ——— : Quasistatic

Fig. 8. Frequency dependence of the characteristic impedances of coupled coplanar waveguides.

Dimensions are the same as in Fig. 7(a).

Fig. 9. Frequency dependence of the effective dielectric constants and the characteristic impedances of coupled coplanar three strips

$\varepsilon_{1xx} = 9.4$, $\varepsilon_{1yy} = 11.6$, $\varepsilon_{1xy} = 0$

$S_{1/h} = 1.0$, $S_{2/h} = 0.5$, $W_{1/h} = 1.5$, $W_{2/h} = 2.0$.

———— : Hybrid-mode, ——— - ——— : Quasistatic

Fig. 10. Effective dielectric constants of coupled coplanar waveguide versus γ.

$\varepsilon_{1xx} = 3.40$, $\varepsilon_{1yy} = 5.12$, $\varepsilon_{1xy} = 0$ when $\gamma = 0$

$S_{1/h} = 1.0$, $S_{2/h} = 0.5$, $W_{1/h} = 1.5$, $W_{2/h} = 2.0$.

Fig. 11. The i-th layer of stratified anisotropic substrates.

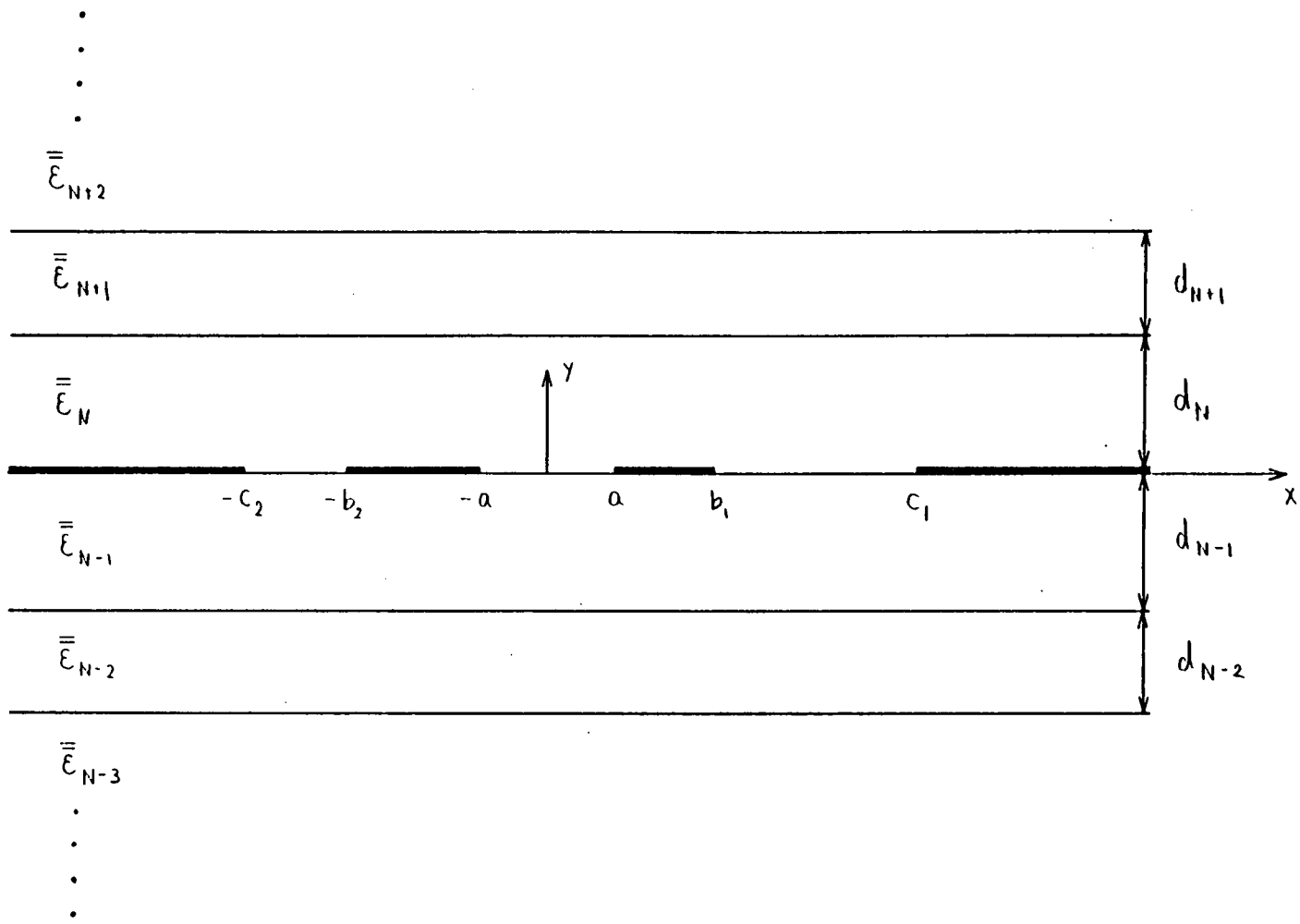

Fig.1 General structure of asymmetrical coupled coplanar-type transmission lines with anisotropic substrates.

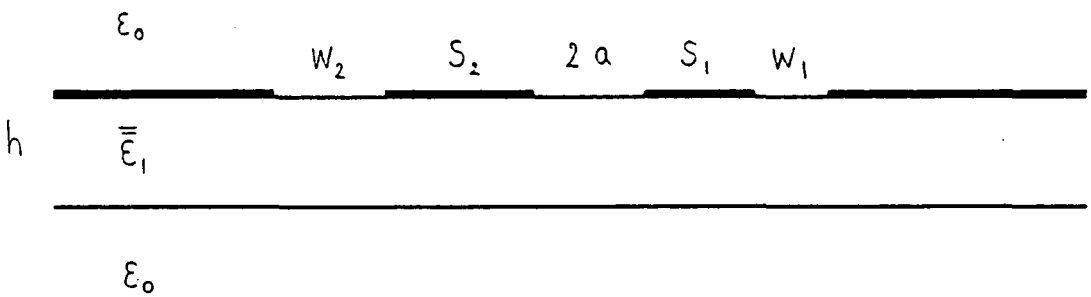
ε_0
W_2
S_2
$2a$
S_1
W_1
h
$\bar{\bar{\varepsilon}}_1$
ε_0

(a)

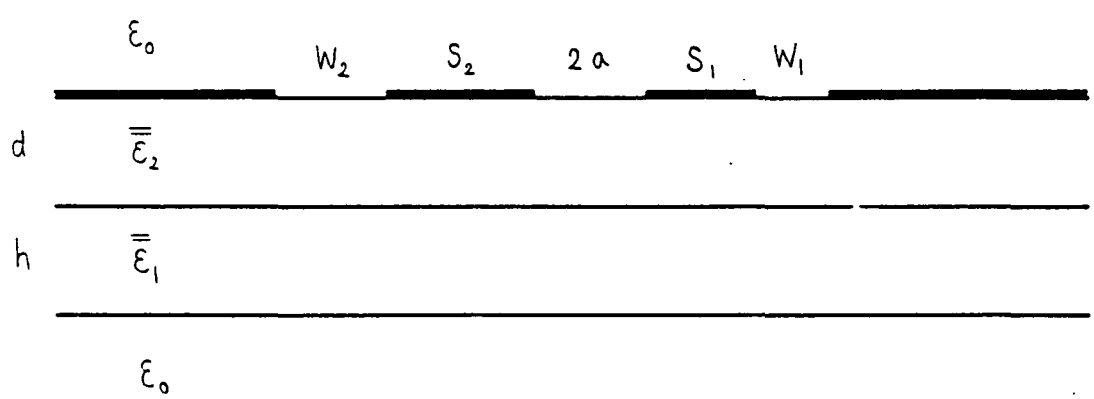
ε_0
W_2
S_2
$2a$
S_1
W_1
d
$\bar{\bar{\varepsilon}}_2$
h
$\bar{\bar{\varepsilon}}_1$
ε_0

(b)

Fig.2

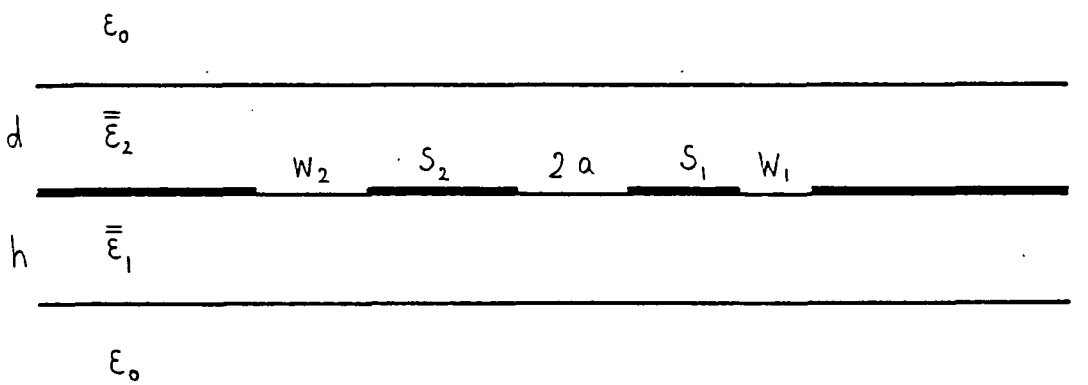

(c)

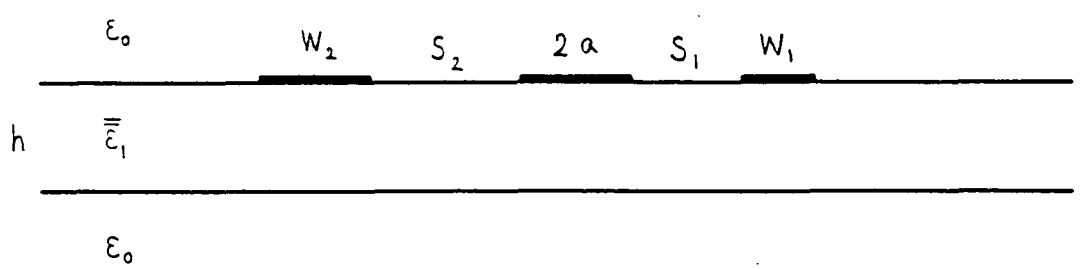

(d)

Fig.2 (a) Asymmetrical coupled coplanar waveguide (C-CPW).

Fig.2 (b) Asymmetrical coupled coplanar waveguide with double-layer substrate .

Fig.2 (c) Asymmetrical coupled sandwich coplanar waveguide.

Fig.2 (d) Asymmetrical coupled coplanar three-strips.

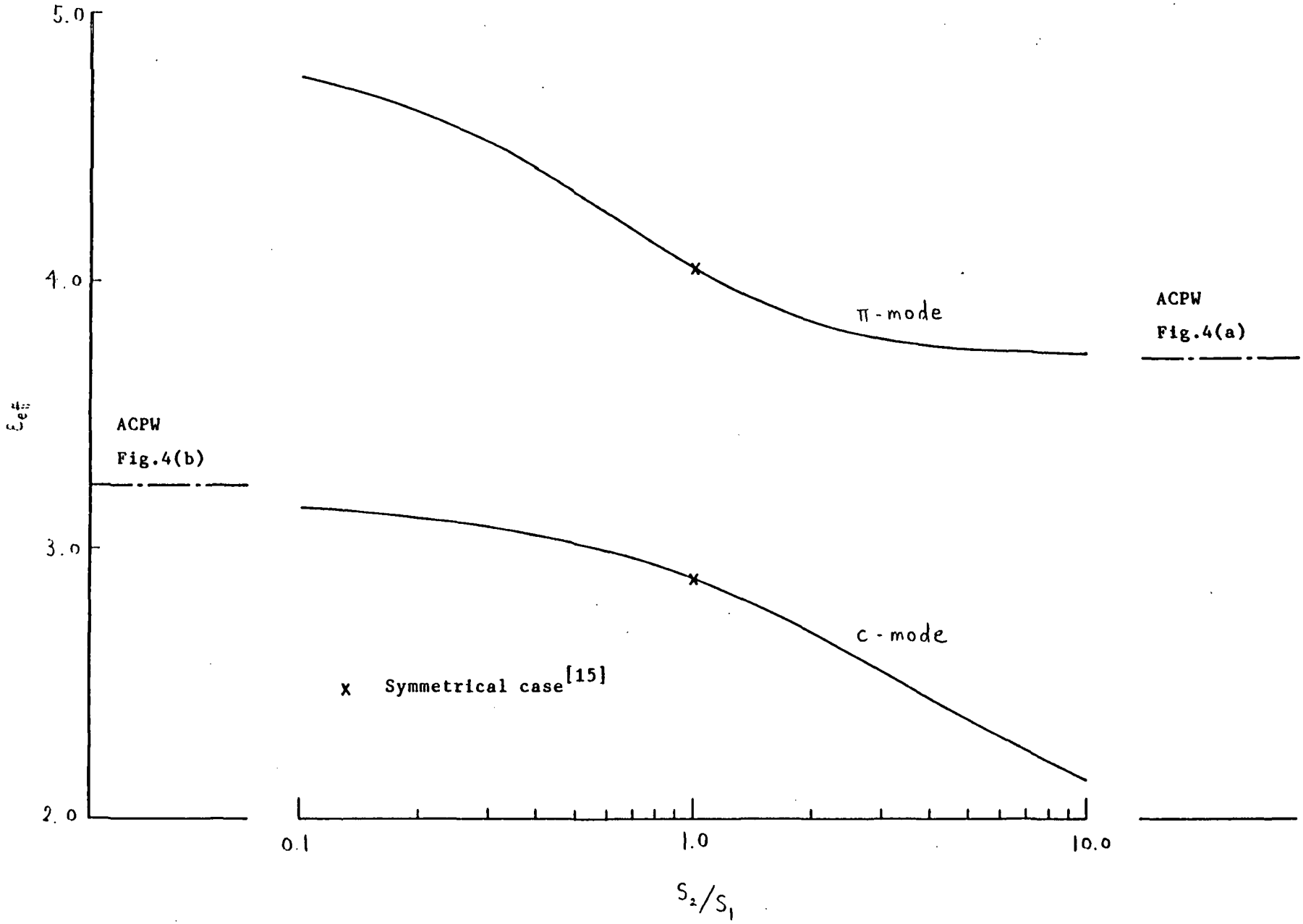
5.0
4.0
3.0
2.0
ε_{eff}
ACPW
Fig.4(b)
ACPW
Fig.4(a)
π-mode
c-mode
x Symmetrical case[15]
0.1
1.0
10.0
S_2/S_1

Fig.3 (a)

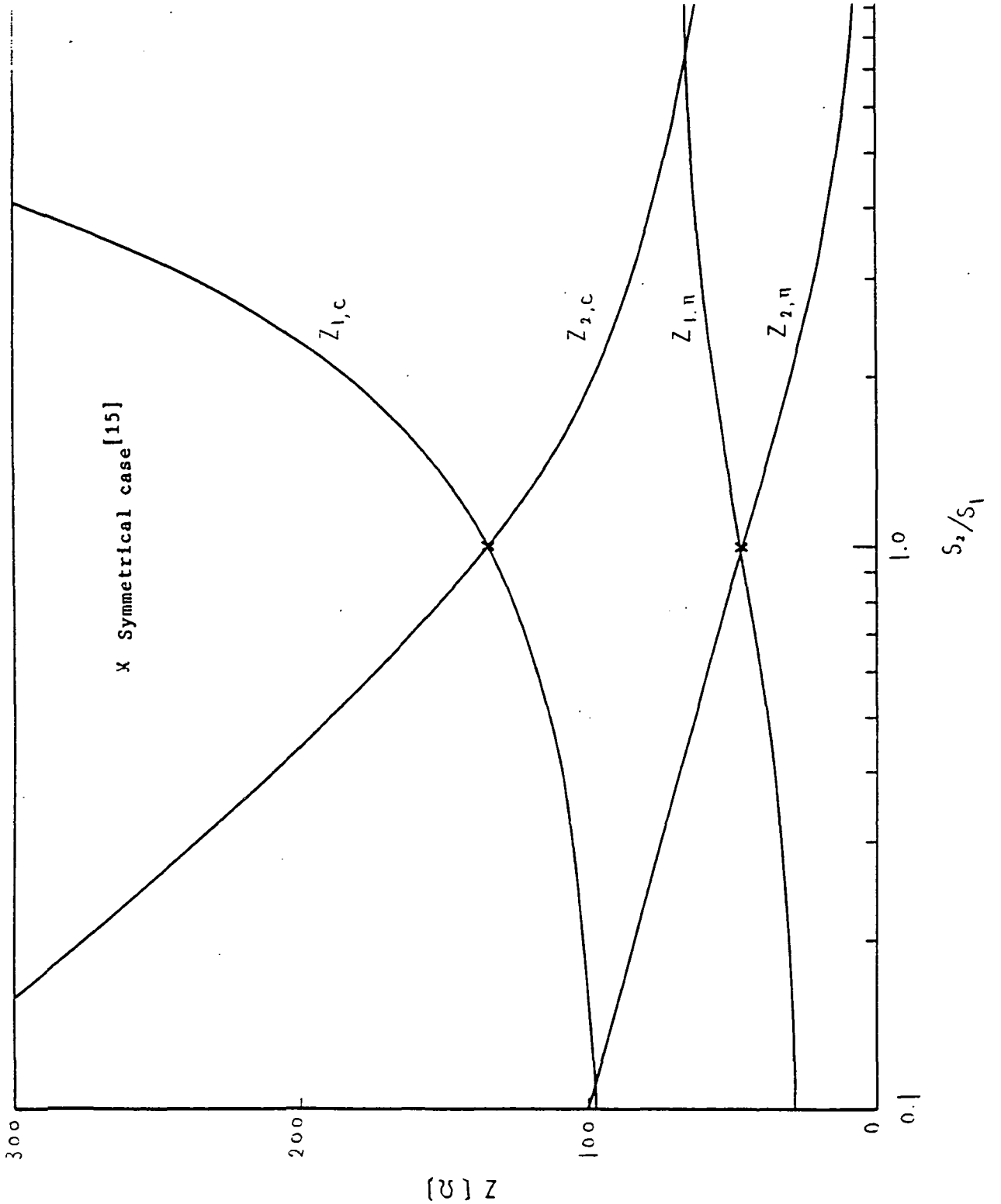

Fig.3 (b)

Fig.3 Quasistatic characteristics of asymmetrical coupled coplanar waveguide versus strip-width ratio S_2/S_1.

(a) Effective dielectric constants

(b) Characteristic impedances

$\varepsilon_{1xx} = \varepsilon_{1yy} = 9.6$, $\varepsilon_{1xy} = 0$

$2a/h = 1$, $S_{1/h} = 2$, $W_{1/h} = 2$, $W_{2/h} = 2$

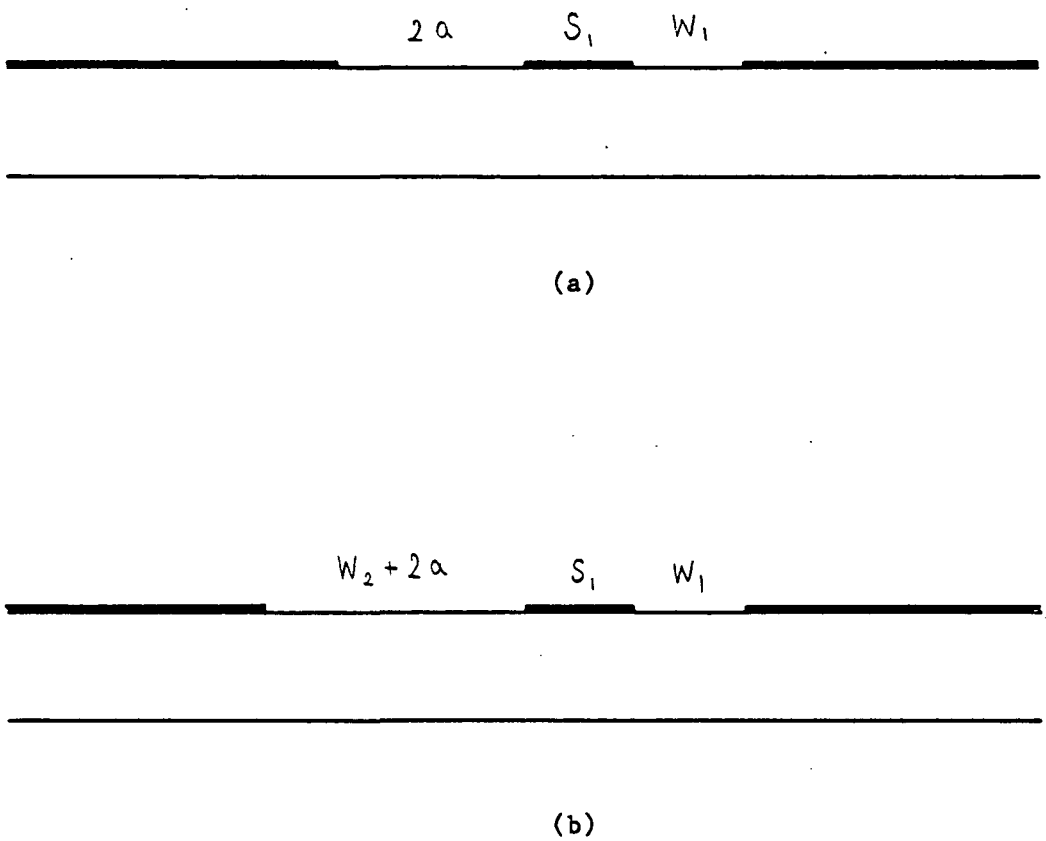

Fig.4 Asymmetrical coplanar waveguide (ACPW).

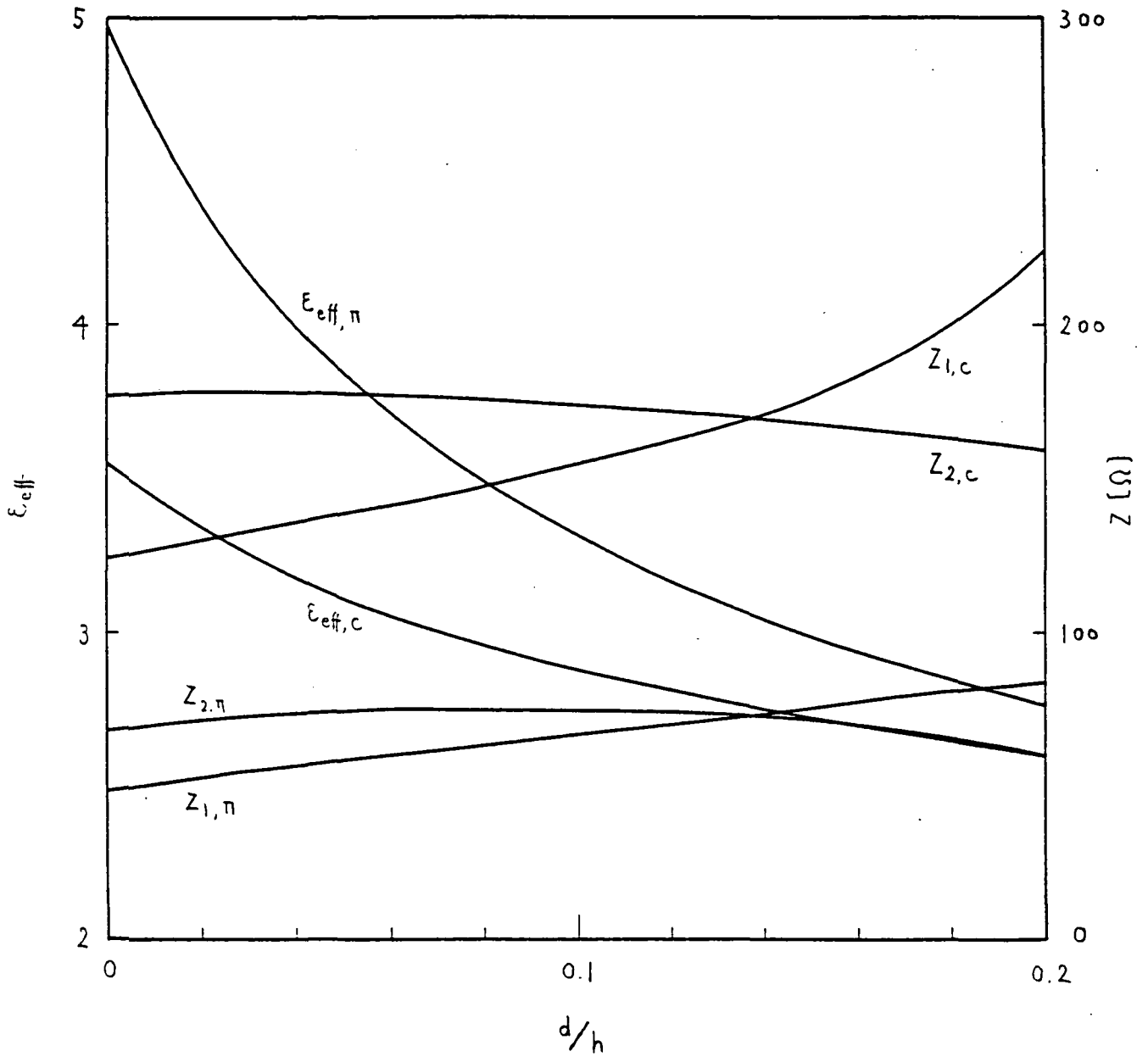

Fig.5 Quasistatic characteristics of asymmetrical coupled coplanar waveguide with double-layer substrate.

$\varepsilon_{1xx} = 9.4$, $\varepsilon_{1yy} = 11.6$, $\varepsilon_{2xx} = \varepsilon_{2yy} = 2.6$,

$\varepsilon_{ixy} = 0$ (i = 1, 2)

$S_{1/h} = 1.0$, $S_{2/h} = 0.5$, $W_{1/h} = 1.5$, $W_{2/h} = 2.0$

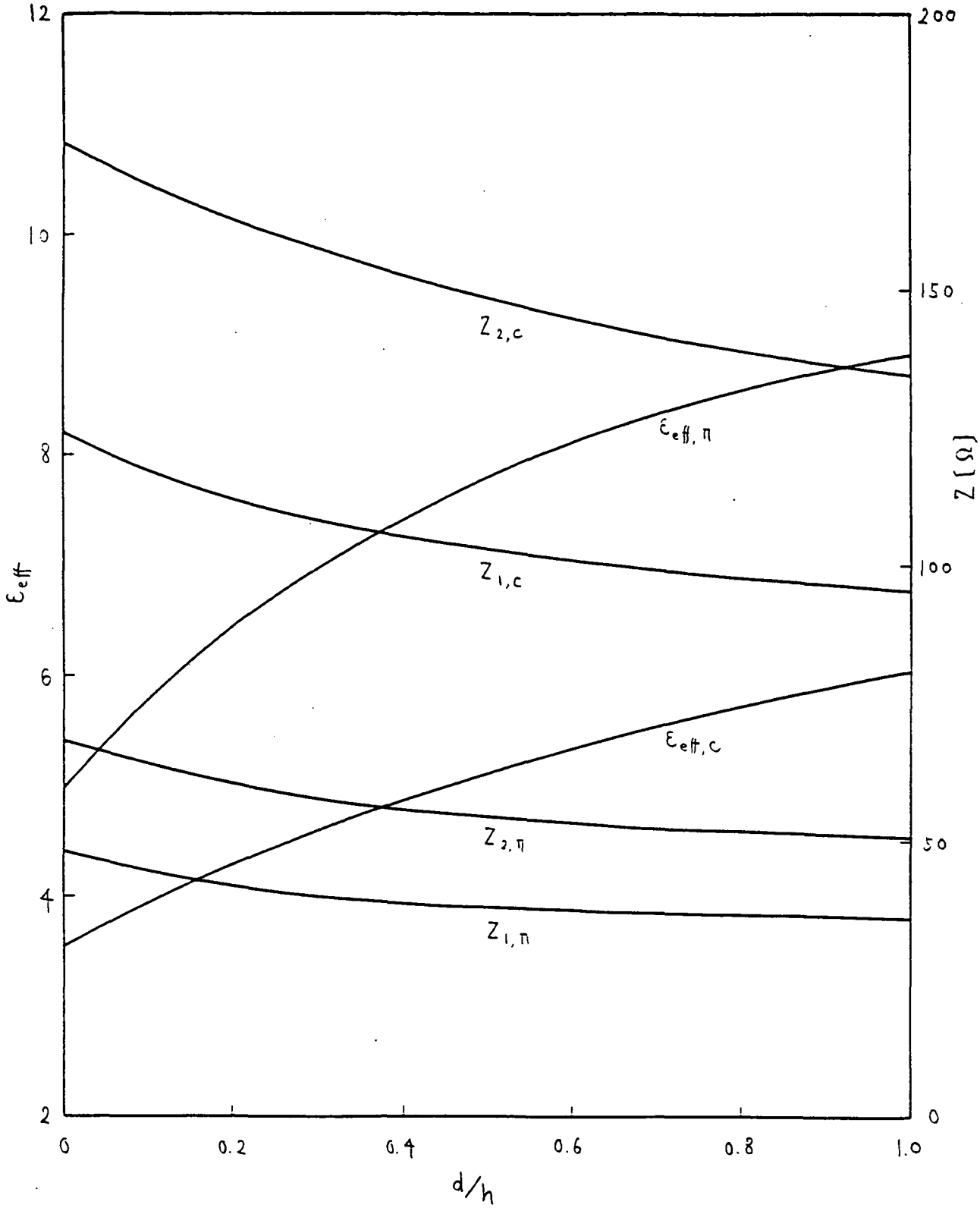

Fig.6 Quasistatic characteristics of asymmetrical coupled sandwich coplanar waveguide.

$\varepsilon_{1xx} = \varepsilon_{2xx} = 9.4$, $\varepsilon_{1yy} = \varepsilon_{2yy} = 11.6$, $\varepsilon_{ixy} = 0$ (i = 1, 2)

$S_{1/h} = 1.0$, $S_{2/h} = 0.5$, $W_{1/h} = 1.5$, $W_{2/h} = 2.0$

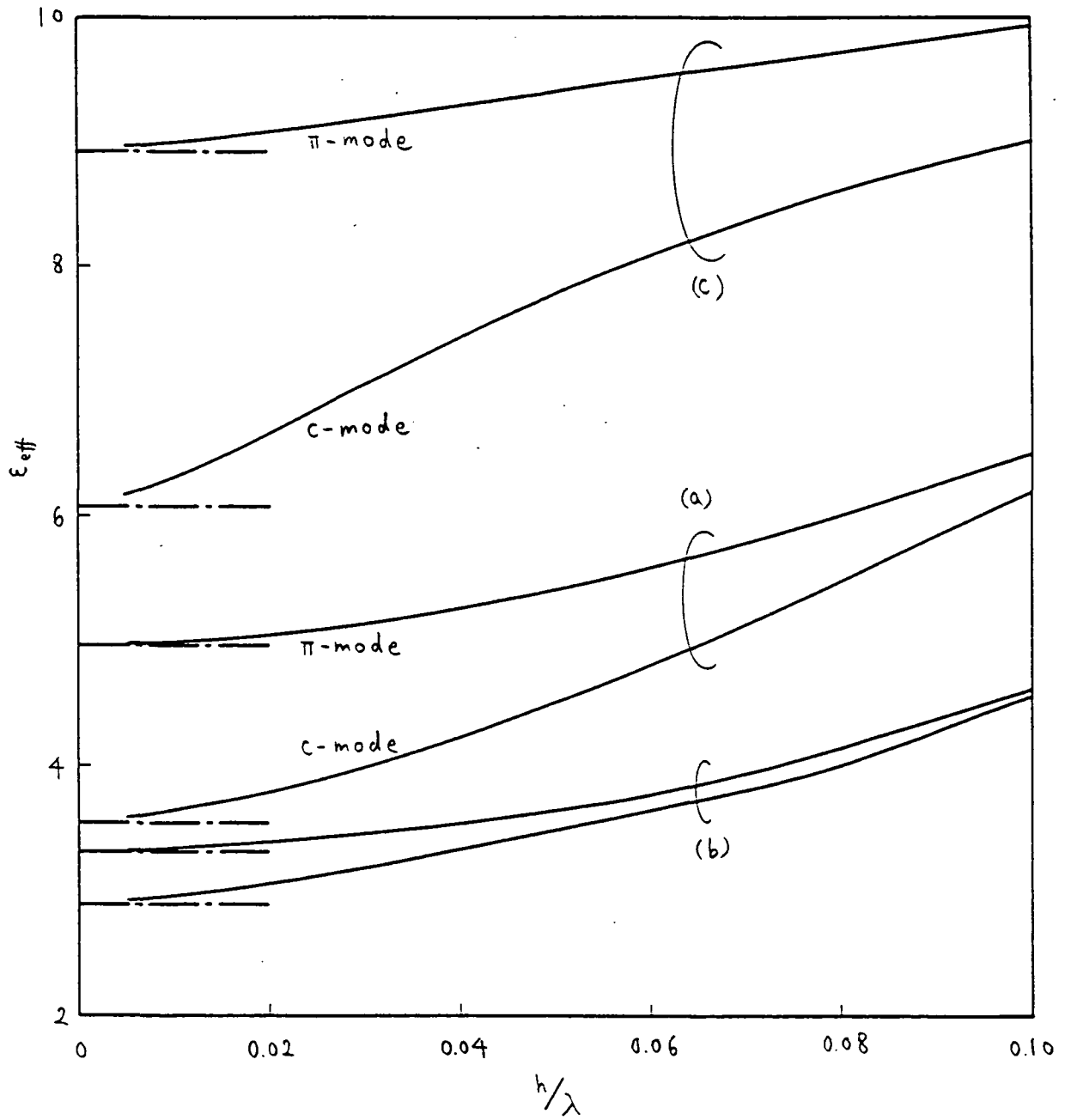
10
8
6
4
2
ε_{eff}
0
0.02
0.04
0.06
0.08
0.10
h/λ
π-mode
c-mode
(c)
(a)
π-mode
c-mode
(b)

Fig.7

Fig.7 Dispersion characteristics of various types of coupled coplanar waveguide.

$S_{1/h} = 1.0$, $S_{2/h} = 0.5$, $W_{1/h} = 1.5$, $W_{2/h} = 2.0$

(a) Asymmetrical coupled coplanar waveguide (C-CPW).

$\varepsilon_{1xx} = 9.4$, $\varepsilon_{1yy} = 11.6$, $\varepsilon_{1xy} = 0$

(b) Asymmetrical coupled coplanar waveguide with double-layer substrate .

$\varepsilon_{1xx} = 9.4$, $\varepsilon_{1yy} = 11.6$, $\varepsilon_{2xx} = \varepsilon_{2yy} = 2.6$,

$\varepsilon_{ixy} = 0$ ($i = 1, 2$) , $d/h = 0.1$

(c) Asymmetrical coupled sandwich coplanar waveguide.

$\varepsilon_{1xx} = \varepsilon_{2xx} = 9.4$, $\varepsilon_{1yy} = \varepsilon_{2yy} = 11.6$,

$\varepsilon_{ixy} = 0$ ($i = 1, 2$) , $d/h = 1.0$

———— : Hybrid-mode, ——— - ——— : Quasistatic

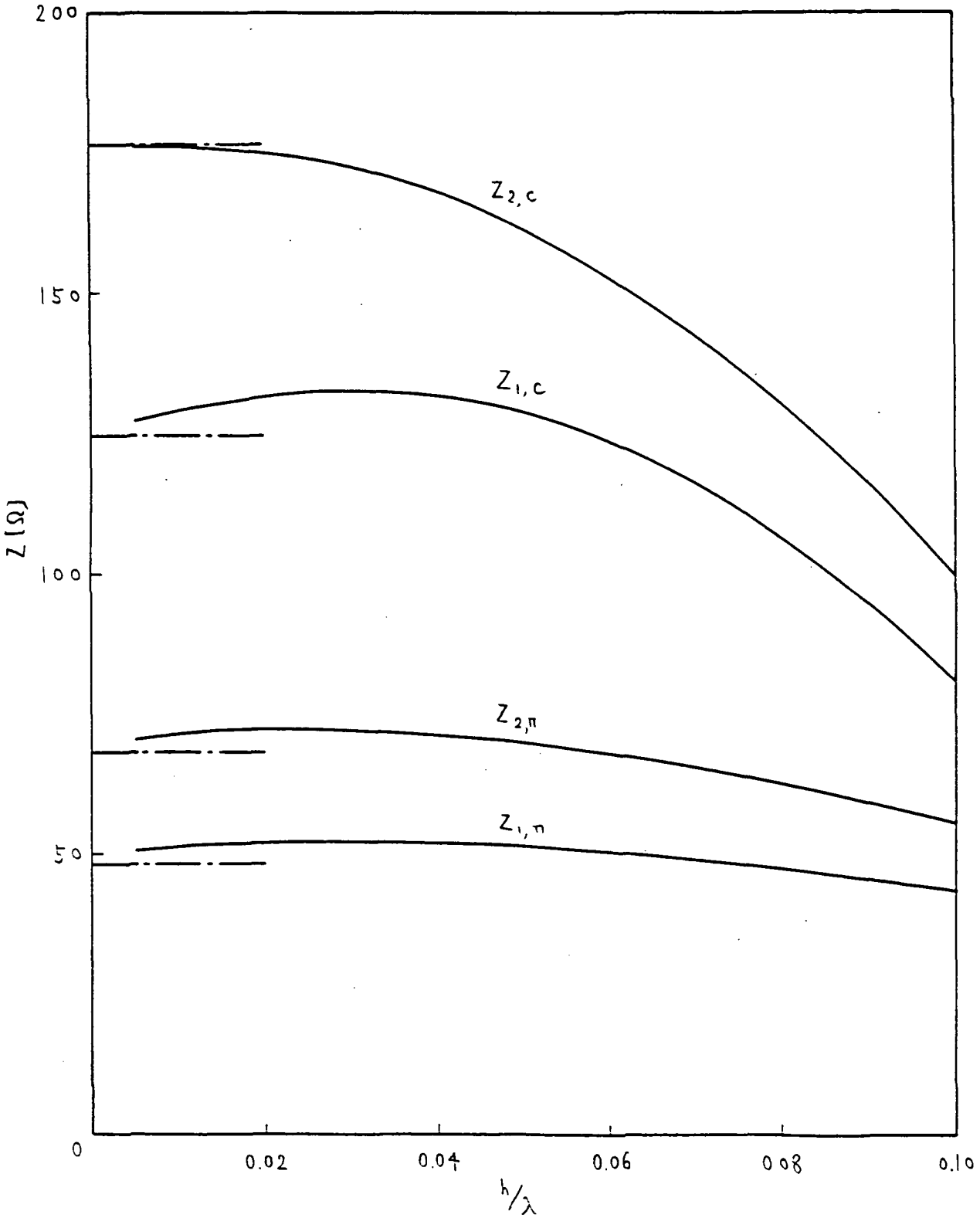

Fig.8 Frequency dependence of the characteristic impedances of coupled coplanar waveguide

Dimensions are same as in Fig.7(a).

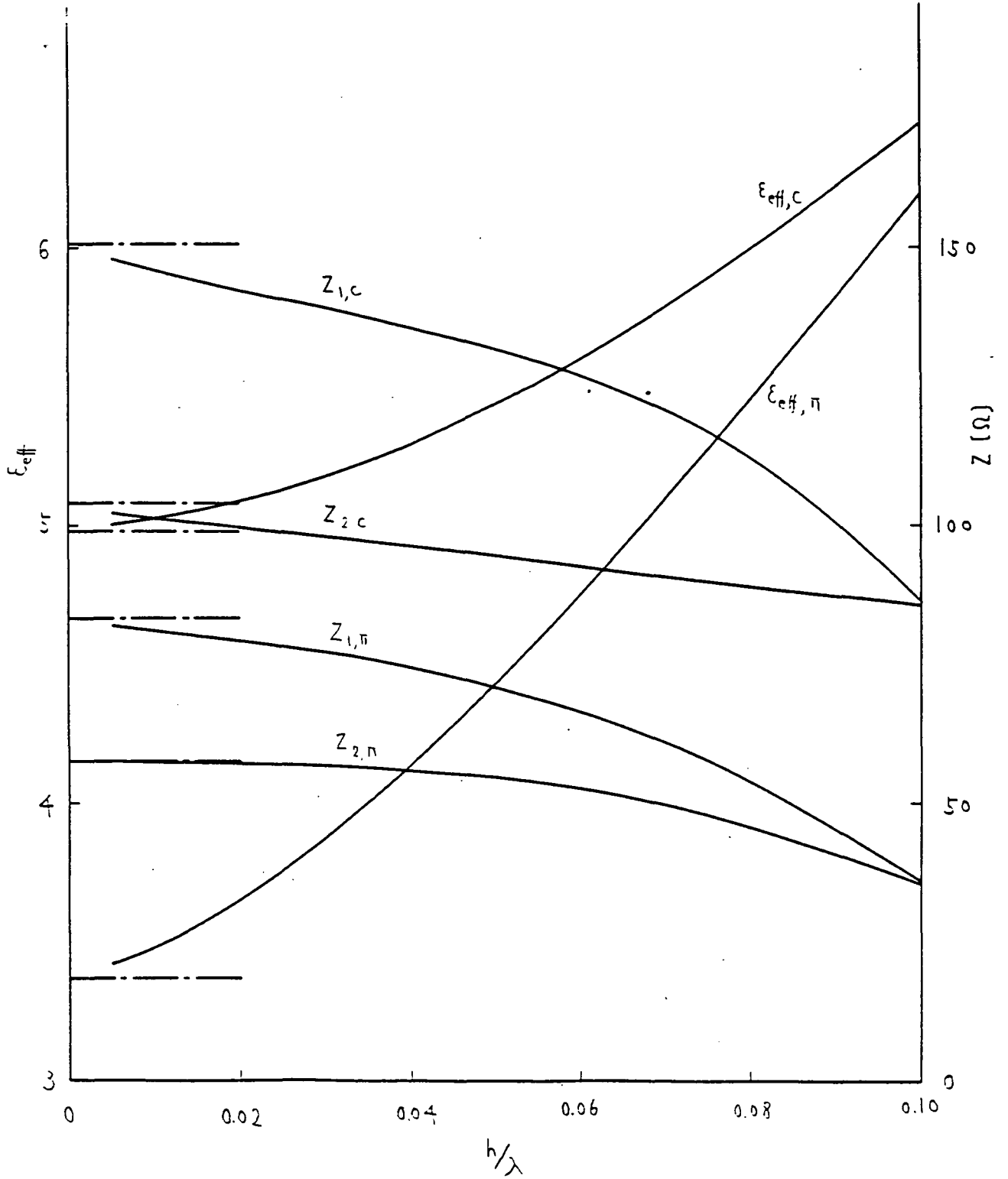

Fig.9 Frequency dependence of the effective dielectric constants and the characteristic impedances of coupled coplanar three-strips

$\varepsilon_{1xx} = 9.4$, $\varepsilon_{1yy} = 11.6$, $\varepsilon_{1xy} = 0$

$S_{1/h} = 1.0$, $S_{2/h} = 0.5$, $W_{1/h} = 1.5$, $W_{2/h} = 2.0$

———— : Hybrid-mode, ——-—— : Quasistatic

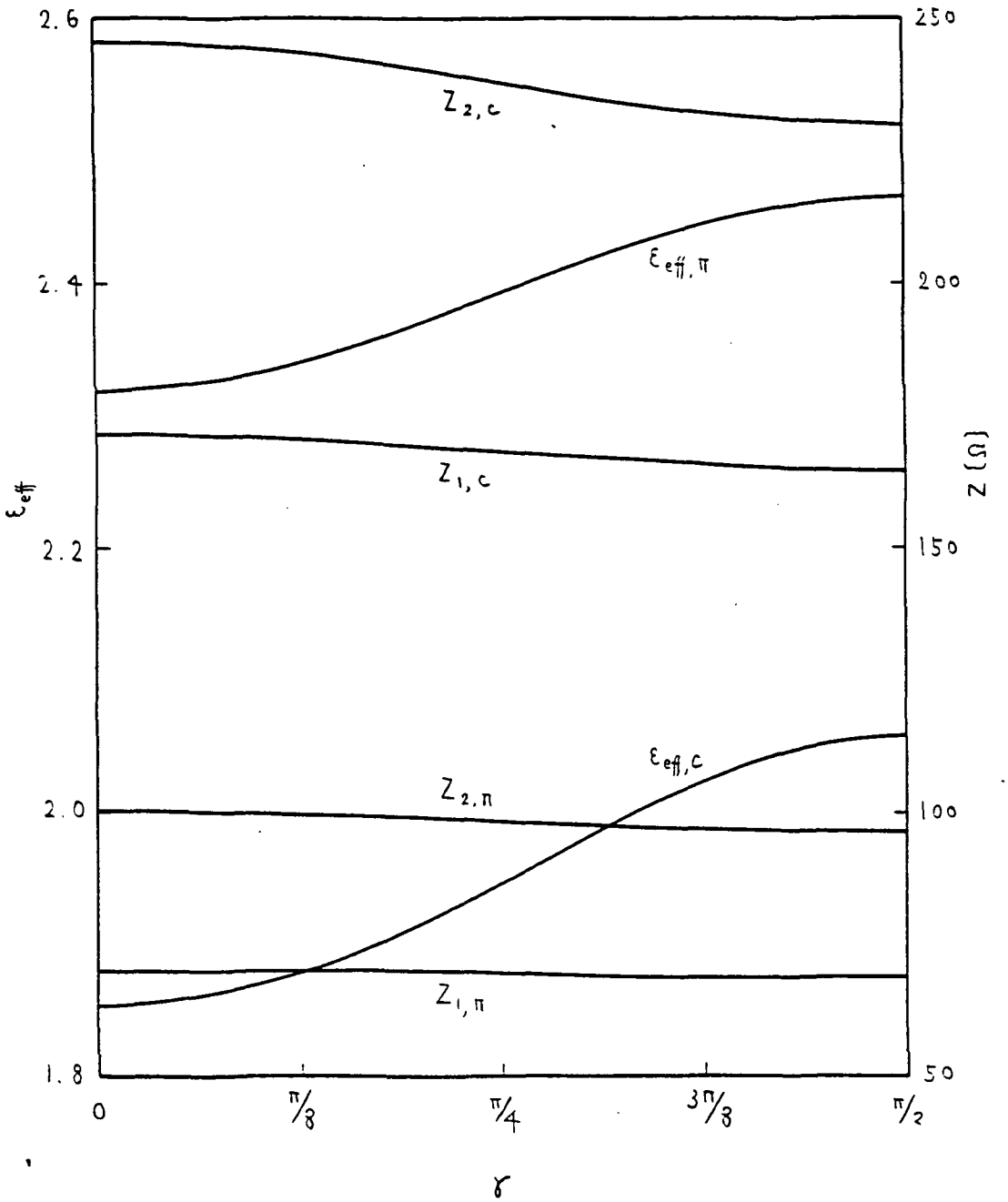

Fig.10 Effective dielectric constants of coupled coplanar waveguide versus γ.

$\varepsilon_{1xx} = 3.40$, $\varepsilon_{1yy} = 5.12$, $\varepsilon_{1xy} = 0$ when $\gamma = 0$

$S_{1/h} = 1.0$, $S_{2/h} = 0.5$, $W_{1/h} = 1.5$, $W_{2/h} = 2.0$

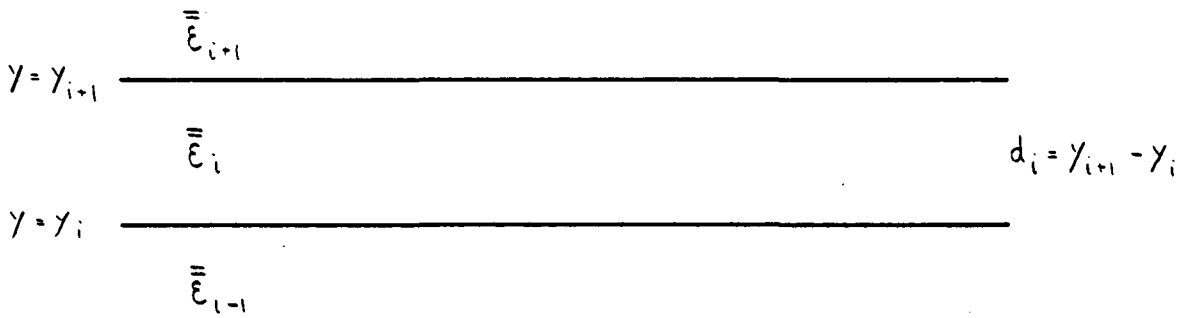

Fig.11 The i-th layer of stratified anisotropic substrates